

Link alla versione pubblicata:

<https://www.sciencedirect.com/science/article/pii/S0016699520300280>

Coralline algae as depth indicators in the Miocene carbonates of the Eratosthenes Seamount (ODP Leg 160, Hole 966F)

Giovanni Coletti^{*}, Daniela Basso

Department of Earth and Environmental Sciences, University of Milano-Bicocca, Piazza della Scienza 4, 20126, Milano, Italy

The abundance of the major coralline algal groups has been investigated and quantified in the coralline-rich facies of the Miocene shallow-water carbonates of the Eratosthenes Seamount (eastern Mediterranean, off-shore Cyprus). The analysis is based on the quantification of the most easily-recognizable groups of coralline algae in order to provide a user-friendly approach for palaeobathymetric reconstructions. Coralline algal distribution through the core suggests water depth estimates generally similar to those based on the composition of the skeletal assemblage and the benthic foraminiferal association in particular. The only noticeable difference occurs in the rhodolith and coral facies, where algal distribution suggests deeper waters than those indicated by benthic foraminifera. The distribution pattern of the major groups suggests that the ratio between Hapalidiales and Corallinales is the most reliable indicator of water-depth. The comparison with other models available in literature highlights a general zonation useful for the study of tropical, middle to late Miocene oligotrophic carbonates. Very shallow settings (0–20 m) are overwhelmingly dominated by Corallinales; in slightly deeper settings (20–40 m) Hapalidiales are more abundant, especially if the sea-floor is shaded (for example by a macrophyte canopy). Between 40 and 60 m, Hapalidiales dominate but Corallinales are still common, while below 60 m Corallinales are very rare. In non-oligotrophic environments this zonation is not reliable and, due to the reduced water clarity related to the high primary productivity, Hapalidiales clearly dominate even in very shallow settings.

1. Introduction

Water depth is one of the most relevant variable in oceanic palaeoenvironmental reconstructions (Perrin et al., 1995). Except for rare instances in which elements indicating absolute water depth (like a preserved reef-flat complex; e.g., Perrin, 2000; Benisek et al., 2009) are available, palaeobathymetric reconstructions are based on biological and sedimentological proxies which are just related to water depth. Grain size, sorting and the distribution of certain groups of organisms are connected to hydrodynamic energy, which generally decreases with increasing water depth. The distributions of algae and of symbiont-bearing organisms (like corals and several groups of benthic foraminifera) are instead mainly controlled by light availability, which decreases with increasing water depth. These apparently simple relationships can be remarkably complicated by factors like down-slope

transport of shallow-water material (Nebelsick et al., 2001; Rasser and Nebelsick, 2003; Checconi et al., 2010; Cipriani et al., 2019), water clarity and nutrient availability (Brasier, 1995a, b; Halfar et al., 2004; Wilson and Vecsei, 2005), and internal waves (Pomar et al., 2012).

Coralline algae are a common component of Cenozoic shelves (Aguirre et al., 2000; Braga et al., 2010; Riosmena-Rodríguez, 2017). Since light availability and hydrodynamic energy are major controls on their distribution and growth form (Sañé et al., 2016), corallines are a useful instrument for palaeobathymetric reconstructions (Iryu, 1992; Bucur and Filipescu, 1994; Bassi, 1998; Cabioch et al., 1999; Braga and Aguirre, 2001, 2004; Brandano et al., 2005, 2007; Kroeger et al., 2006; Barattolo et al., 2007; Benisek et al., 2009; Braga et al., 2009; Quaranta et al., 2012; Bracchi et al., 2014; Vescogni et al., 2014; Coletti et al., 2018a; Chelaru et al., 2019). However, their use is hampered by the insufficient information on their present-day depth distribution in many regions of the world and their complex taxonomic history. Coralline algae depth distribution was mainly investigated during the last decades of the twentieth century (Adey and Macintyre,

1973; Van Den Hoek et al., 1975; Adey, 1979, 1986; Adey et al., 1982; Noro et al., 1983; Minnery et al., 1985; Perrin et al., 1995; Iryu, 1992; Iryu et al., 1995; Rasser and Piller, 1997; Basso, 1998; Cabioch et al., 1999; Lund et al., 2000), but nowadays the research is more focused on their potential as palaeoclimatic archives. Molecular genetics radically revised the knowledge of coralline algae taxonomy, discovering a previously unknown cryptic diversity and revolutionizing higher-rank taxonomy (Harvey et al., 2003; Le Gall et al., 2009; Adey et al., 2015; Nelson et al., 2015; Van Der Merwe et al., 2015). Coralline-algal paleontology also improved by embracing many of the changes proposed by modern phycology (Braga et al., 1993; Braga and Aguirre, 1995; Basso et al., 1996, 1998; Rasser and Piller, 1999, 2000; Woelkerling et al., 2014; Hrabovský et al., 2015; Chelaru and Bucur, 2016; Coletti et al., 2016; Hrabovský, 2019). Although this revolution greatly improved our knowledge of corallines, keeping a unique taxonomy for living and fossil corallines is becoming more and more challenging, because of the difficulties in identifying diagnostic sets of morphological characters (which often have a limited fossilization potential) that support the observed genetic diversity.

This paper investigates the coralline algal distribution as a tool for palaeodepth reconstruction along the Miocene shallow-water carbonates of the Eratosthenes Seamount (ODP leg 160; Hole 966F), by thin-section quantification of easily-recognizable groups of coralline algae (Coletti et al., 2018a). This approach aims to provide a tool that is accessible to the non-specialist, that can be used even when preservation is far from optimal, and that allows for broad-scale comparisons. The Eratosthenes Seamount is the highest preserved elevation of a fragment of continental crusts detached from North Africa during the Mesozoic. It is characterized by a thick carbonate sedimentary cover that developed for millions of years protected from terrestrial influx (Mart and Robertson, 1998; Premoli-Silva et al., 1998; Robertson, 1998a, b, c; Montadert et al., 2014) (Fig. 1). This succession recorded the environmental evolution of the Eastern Mediterranean region during the Miocene, while the (palaeo)Mediterranean Basin was turning from a large seaway connecting the Indo-Pacific with the Atlantic to its modern state of semi-enclosed basin (Robertson and Dixon, 1984; Rögl, 1999; Dercourt et al., 2000; Cornacchia et al., 2018). The stratigraphy and the palaeoenvironmental interpretation of these shallow-water carbonates have been recently updated (Coletti et al., 2019; Fig. 1), making this unique succession an interesting test area to assess the usefulness of coralline algae as depth indicators.

2. Geological settings

The basement of the Eratosthenes Continental Block is probably composed of thinned continental crust with mafic intrusions related to the rifting (Robertson, 1998c; Ben-Avraham et al., 2002; Montadert et al., 2014). The sedimentary cover investigated by ODP Leg 160, Sites 965, 966 and 967, consists of Aptian (or possibly older) to Late Cretaceous shallow-water carbonates, pelagic chalks of Cenomanian to Paleogene age, Miocene shallow-water carbonates, various deposits related to the Messinian Salinity Crisis, and Pliocene to recent deep-water sediments (Emeis et al., 1996; Major et al., 1998; Premoli-Silva et al., 1998; Robertson, 1998a, b; Spezzaferri et al., 1998; Spezzaferri and Tamburini, 2007; Coletti et al., 2019) (Fig. 1(C)). Cretaceous shallow-water limestones are characterized by pellets, small benthic foraminifera (mainly miliolids), ostracods, calcareous algae and echinoderms, testifying to a shallow-water environment interpreted as a lagoon (Premoli-Silva et al., 1998; Robertson, 1998a). The overlying chalks are mainly dominated by planktonic foraminifera but they present

also layers rich in crinoid fragments and chert nodules; they are locally enriched in organic matter (Robertson, 1998a). These rocks formed in a deep-water setting occasionally affected by deep-water currents (Robertson, 1998a). Organic rich intervals are probably related to events of increased productivity or of reduced circulation (Robertson, 1998a; Meilijson et al., 2014, 2015). On the summit of the seamount a major hiatus (Bartonian to early Miocene in Hole 966F; Staerker, 1998; Coletti et al., 2019), separates pelagic chalks from Miocene shallow-water carbonates. Large grains of glaucony characterize this boundary, indicating a prolonged period of reduced sedimentation or of non-deposition (Major et al., 1998; Robertson, 1998a; Coletti et al., 2019).

Three main intervals and six facies were recognized in the Miocene shallow-water carbonates (Coletti et al., 2019; Fig. 1(C)). The lowermost interval has been attributed to the early Miocene on the basis of large benthic foraminiferal associations (Coletti et al., 2019). The skeletal assemblage is dominated by lepidocyclinids, miogypsinids and echinoid fragments, with common planktonic foraminifera (especially at the base of the interval) and rare bryozoans and coralline algae (Coletti et al., 2019; Fig. 1(C)). The central interval has been tentatively dated to the middle Miocene (based on the first occurrence of *Orbulina universa* and the disappearance of lepidocyclinids and miogypsinids; Coletti et al., 2019; Fig. 1(C)). From the base to the top, the central interval is characterized by a facies rich in rhodoliths and corals, overlain by a facies dominated by heterosteginids and coralline algae related to a macrophyte meadow and by a top layer once again rich in rhodoliths and corals (Coletti et al., 2019; Fig. 1(C)). The uppermost interval has been dated as late Miocene on the basis of Sr isotopes stratigraphy; from the base to the top, it is characterized by a coral-reef facies with hermatypic corals and coralline algae and a by a facies dominated by mollusks and benthic foraminifera (mainly miliolids) which indicates a lagoonal environment (Coletti et al., 2019; Fig. 1(C)). The transition from pelagic chalks to shallow-water carbonates that occurred at the base of the Miocene succession testifies to a major shallowing upward. This is related to the regional collision of the Eurasian (Anatolian) and African plates that caused the uplift of the subducting plate, probably through the mechanism of peripheral bulge uplift (Forsyth, 1980; Jacobi, 1981).

Miocene shallow-water carbonates are overlain by brackish and sub-aerial deposits related to the Messinian Salinity Crisis (Major et al., 1998; Robertson, 1998d; Coletti et al., 2019), which in turn are covered by Zanclean pelagic sediments (Major et al., 1998; Spezzaferri and Tamburini, 2007; Fig. 1(C)). The Plio-Pleistocene succession records further subsidence (Spezzaferri and Tamburini, 2007). The subsidence started during the late Pliocene, being driven by the collision and subduction of the Eratosthenes Seamount below Cyprus, and is coupled with the rapid uplift of the island (Robertson et al., 1991; Robertson, 1998c; Kinnaird et al., 2011; Kinnaird and Robertson, 2013; Feld et al., 2017; Murray and Robertson, 2020).

3. Material and methods

Coralline algae have been investigated in the central and upper intervals of the Miocene shallow-water succession (Coletti et al., 2019), following the approach proposed by Coletti et al. (2018a), based on the thin section quantification of easily recognizable coralline algal groups. In the lower interval, coralline algae are rare and core-recovery is extremely low (Emeis et al., 1996; Coletti et al., 2019). Consequently, there was not enough material to perform a detailed analysis of coralline-algal flora. Water depth estimations proposed in Coletti et al. (2019) are chiefly based on the skeletal assemblages and on benthic foraminiferal associations; therefore, they are suitable to test coralline algae as depth indicators.

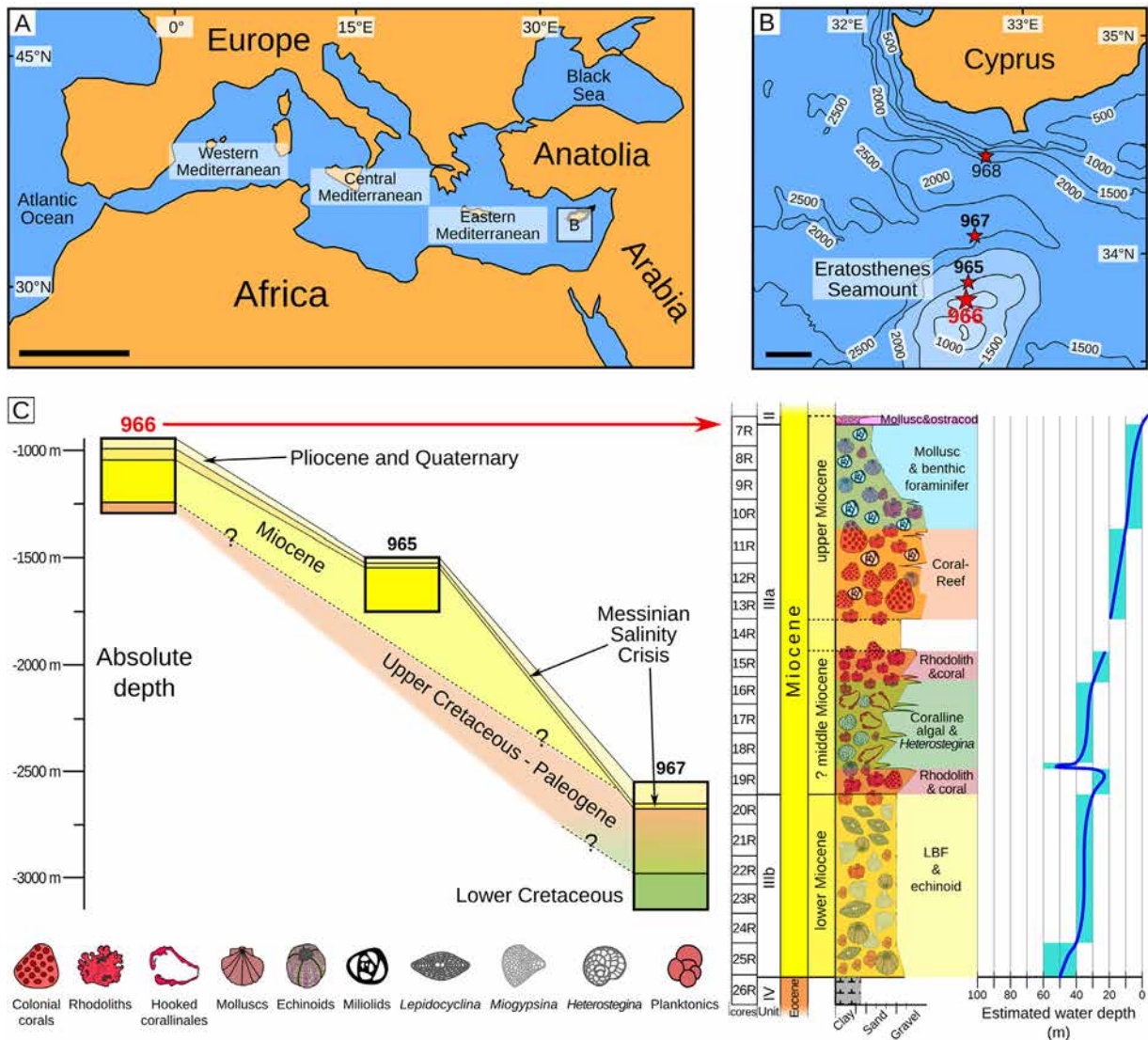


Fig. 1. Study area. **A.** Map of the modern Mediterranean region. **B.** Map of the area of the Eratosthenes Seamount, indicating the position of the Holes drilled by ODP Leg 160, modified from Robertson (1998a). **C.** Stratigraphic section across the Eratosthenes Seamount, showing the successions recovered at Sites 965, 966 and 967, and their water depths, modified from Mart and Robertson (1998); on the right is given the lithostratigraphic column of the Miocene shallow-water carbonates, including facies and estimated water depth, modified from Coletti et al. (2019). Scale bars: 1000 km (A), 20 km (B).

The succession of Hole 966F was observed and re-sampled for coralline algae at MARUM–IODP Core Repository in Bremen (Germany); 45 new thin sections were prepared (polished with 1 μm aluminum oxide) (Table 1). Coralline algal abundance in thin sections was quantified using the open-source vector-graphic editor Inkscape (release 0.91 for Ubuntu). The algae were identified under light microscope and then the thin sections were scanned (Fig. 2). The raster image was imported in Inkscape and the outlines of the specimens were traced using the vector graphic editor. Specimens' area was measured (in px^2 , later converted in mm^2) using the path-measuring extension of the program (Fig. 2).

Rhodoliths description follows Bosence (1983a). The growth-form terminology used here follows Woelkerling et al. (1993), while the terminology for the vegetative anatomy follows Hrabovský et al. (2015), using hypothallus and perithallus as synonyms for ventral core of basal filaments and peripheral zone, respectively (Fig. 3(A)). The vegetative anatomy was studied along radial sections (Quaranta et al., 2007; Vannucci et al., 2008), and the diameter and length of the cells were measured including cell walls (Basso et al., 1996; Fig. 3(A)). Reproductive anatomy was also

investigated in radial sections. Uniporate conceptacles were measured along the section that cuts through the central part of the cavity, resulting in the pore canal being completely visible, Afonso-Carrillo et al. (1984) (Fig. 3(B–D)).

In the recent years, higher rank-taxonomy of coralline algae has been changing at an astonishing pace, resulting in the impossibility to compare data-sets produced under different taxonomic frameworks. In order to allow a proper comparison with previously published results (following an approach similar to the one of other palaeontological papers, e.g., Aguirre et al., 2000), we decided to ignore some of the most recent taxonomic updates based on molecular genetics and use a simplified higher-rank scheme consisting of three major groups, easily recognizable on the basis of the reproductive anatomy:

- coralline algae with sporangial thalli characterized by uniporate conceptacles (Corallinales *sensu* Rösler et al., 2016; Fig. 3(B));
- coralline algae with sporangial thalli characterized by multiporate conceptacles (Hapalidiales *sensu* Nelson et al., 2015; Fig. 3(C));

Table 1

Position of the examined samples within Hole 966F. R stands for rotary core; CC stands for core catcher; W stands for working half. The thin section code is used to identify the thin sections created from the sample; the same coding is used in Table S1 (Appendix A).

Expedition	Site	Hole	Core	Type	Section of the core	Half	Lower boundary of the interval (cm)	Upper boundary of the interval (cm)	Thin section code
160	966	F	7	R	2	W	1	4	7IIaok
160	966	F	7	R	2	W	47	51	7IIb
160	966	F	8	R	1	W	30	34	8I0
160	966	F	9	CC	1	W	6	9	9Ia'
160	966	F	10	R	1	W	114	118	10Ib; 10Ib'
160	966	F	10	R	1	W	119	122	10Ic
160	966	F	10	R	2	W	96	100	10IIb'
160	966	F	10	R	2	W	114	118	10IIc
160	966	F	11	R	1	W	78	81	11Ib
160	966	F	11	R	1	W	113	116	11Ic
160	966	F	11	R	2	W	55	60	11IIa'
160	966	F	11	R	2	W	91	94	11IIb
160	966	F	11	R	3	W	24	28	11III0
160	966	F	11	R	3	W	75	70	11III00
160	966	F	12	R	1	W	30	34	12I0
160	966	F	12	R	1	W	77	79	12I00
160	966	F	13	R	1	W	41	44	13I0
160	966	F	15	R	1	W	74	79	15Ia0
160	966	F	15	R	1	W	104	109	15Ia00
160	966	F	15	R	2	W	8	12	15II0
160	966	F	15	R	2	W	32	36	15IIa'
160	966	F	15	R	2	W	58	62	15IIb
160	966	F	16	R	1	W	142	144	16Ic
160	966	F	16	R	2	W	56	59	16II0
160	966	F	16	R	2	W	122	125	16IIa'
160	966	F	16	R	2	W	147	148	16IIb
160	966	F	16	R	3	W	10	13	16IIIa'
160	966	F	16	R	3	W	92	95	16IIIb
160	966	F	17	R	1	W	24	27	17Ia; 17Ia'
160	966	F	17	R	1	W	66	69	17Ia2
160	966	F	17	R	2	W	1	5	17II0
160	966	F	17	R	2	W	45	48	17II00
160	966	F	17	R	3	W	59	62	17IIIb
160	966	F	17	R	3	W	129	131	17IIIc
160	966	F	17	R	4	W	15	18	17IVa
160	966	F	18	R	2	W	3	7	18IIa
160	966	F	18	R	2	W	71	40	18IIId
160	966	F	19	R	1	W	80	82	19Ib
160	966	F	19	R	1	W	124	127	19Ic
160	966	F	19	R	3	W	54	59	19IIIa0
160	966	F	19	R	3	W	67	72	19IIIa00
160	966	F	19	R	3	W	73	80	19IIIb; 19IIIb'

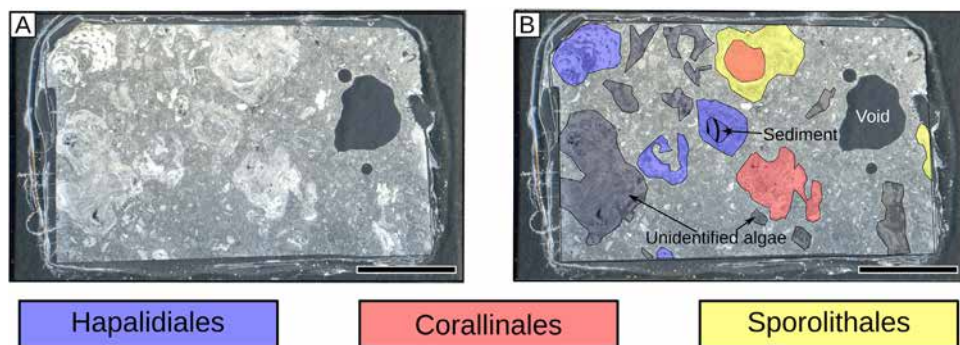


Fig. 2. Corallines surface quantification. **A.** Raster image of a thin section. **B.** The same thin section with the identification of the main groups of coralline algae. Blue: Hapalidiales; Red: Corallinales; Yellow: Sporolithales; Gray: unidentifiable. Scale bars: 1 cm.

- coralline algae with sporangial thalli characterized by sporangi grouped in sori (Sporolithales *sensu* Le Gall et al., 2009; Fig. 3(D)).

This division allows for an easy separation of coralline algae (even in fossil material) and enables comparisons with all previously published data-sets on coralline algae depth distribution, being particularly useful for broad-scale investigations

(through time or across large geographical scales). Among Hapalidiales, the separation of *Phymatolithon* from *Lithothamnion* is based on the shape of the epithallial cells – flared in *Lithothamnion* – and the pattern of cell elongation, which is progressive in *Phymatolithon* and meristematic in *Lithothamnion* (Woelkerling and Irvine, 1986; Basso, 1995; Rasser and Piller, 2000). In cases where the incomplete preservation of epithallial

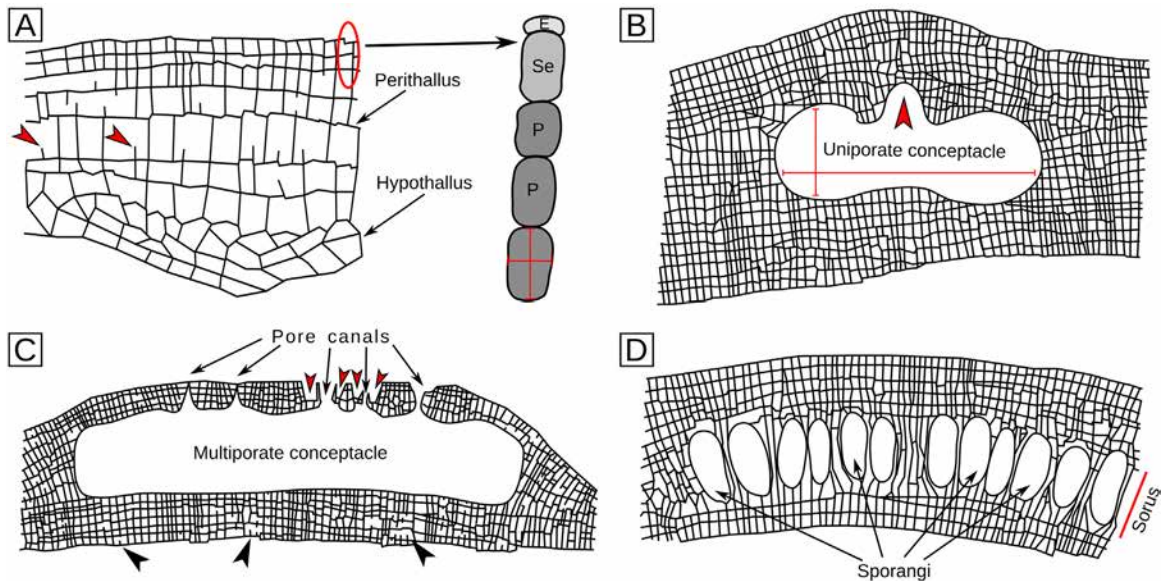


Fig. 3. Diagnostic characters in coralline algae mentioned in this paper. **A.** Vegetative anatomy, indicating hypothallus and perithallus; the represented example is characterized by common cell fusions between contiguous filaments (red arrowheads); on the right, magnification of the uppermost part of the cell filament toward the thallus surface. E: epithallus; Se: subepithallial initial; P: perithallial cells; the red bars indicate cell length and cell diameter. **B.** Reproductive anatomy in Corallinales; the red bars indicate the diameter and height of the uniporate conceptacle; the red arrowhead indicates the completely visible pore canal; the represented example lacks cell fusions between contiguous filaments. **C.** Reproductive anatomy in Hapalidiales; the multiporate conceptacle presents conical pore canals, and pore canals with pits on the outer surface (red arrowheads) which are the diagnostic features of *Lithothamnion crispatum*; as for all Hapalidiales, the represented example presents cell fusions between contiguous filaments (black arrowheads). **D.** Reproductive anatomy in Sporolithales; the represented example lacks cell fusions between contiguous filaments, although that may occur.

and subepithallial cells prevented genus identification, the notation *?Lithothamnion* has been used (following Hrabovský et al., 2015).

The trophic conditions of the palaeoenvironment have been investigated on the basis of the data of SEDEX sequential extraction provided in Coletti et al. (2019). The SEDEX extraction allows an accurate quantification of the five known sedimentary phosphorus reservoirs (Ruttenberg, 1992, 2004; Ruttenberg et al., 2009), i.e., loosely-bound phosphorus, Fe-bound phosphorus, authigenic phosphorus (carbonate-fluoroapatite, biogenic apatite and carbonate bound phosphorus), and detrital apatite and organic phosphorus (Ruttenberg, 2004). Except for detrital apatite, all these reservoirs represent potential sinks for the reactive phosphorus presents into the sea-water (Ruttenberg, 1992). The sum of their contribution (bioavailable-P) is thus related to the nutrient concentration in the palaeoenvironment at the time of sediment formation and can provide information on the trophic conditions (Coletti et al., 2017).

4. Results

Coralline-algal taxa were recognized in 37 thin sections (Table S1; Appendix A). In the remaining 7, coralline algae were either entirely absent, extremely poorly preserved or present in fragments too small to allow any kind of taxonomic identification; for these reasons, these thin sections were excluded from the analysis. The 37 thin sections belong to the rhodolith and coral facies, the coralline algal and *Heterostegina* facies, the coral-reef facies and the mollusk and foraminifer facies. Within these thin sections, 60% of the observed thalli was confidently allocated to one of the three major groups; however, due to the relatively poor preservation of the material, species level identification was not possible in most cases (Table S1; Appendix A).

4.1. Rhodolith and coral facies; 19R-3

This interval is characterized by rhodoliths and fragments of coral colonies associated with a benthic foraminiferal assemblage with common *Amphistegina* and epiphytic foraminifera (mainly *Neoconorbina* but also *Elphidium*), rare *Heterostegina* and very rare planktonic foraminifera (Figs. 4(A–D), 5). Most of the observed rhodoliths show dichotomous branching but laminar specimens also occur (Fig. 4(B)). Both types generally present a compact internal structure (Fig. 4(B)). Fragments of *Porites* have been observed at the core of some of the rhodoliths (Fig. 4(D)). Small branches also occur (Fig. 4(A)). Hapalidiales dominate (63.5%) among the identified algae; Corallinales are common (35%) and Sporolithales s.l. are rare (1.5%) (Figs. 4(E–H), 5).

4.2. Coralline algal and *Heterostegina* facies; 19R-2 to 16R-2

Coralline algae, abundant *Heterostegina* and epiphytic foraminifera characterize this facies (Figs. 5, 6(A)). Coralline algae are mainly represented by thin laminar encrusting thalli with coaxial hypothallus, and thin hooked crusts (both intact and fragmented; Fig. 6(B–E)). Rhodoliths are rare, but in the upper part of the interval (17R-1 to 16R-2) they are more common; conversely, encrusting thalli are less abundant in the upper part. Most of the rhodoliths have a laminar structure and present a rather loose structure (Fig. 6(D)). The large algal structures reported between cores 16R-2 and 16R-3 (Coletti et al., 2019) are composed of loosely arranged crusts locally presenting protuberances with dichotomous branching. Small branches also occur, especially in the upper part of the interval (Fig. 6(E)). Among the identified taxa, Hapalidiales largely dominate (71%); they are especially frequent and common between cores 19R-1 and 17R-1 (Fig. 5). Most of the identifiable thalli belongs to *Lithothamnion* and *Lithothamnion*

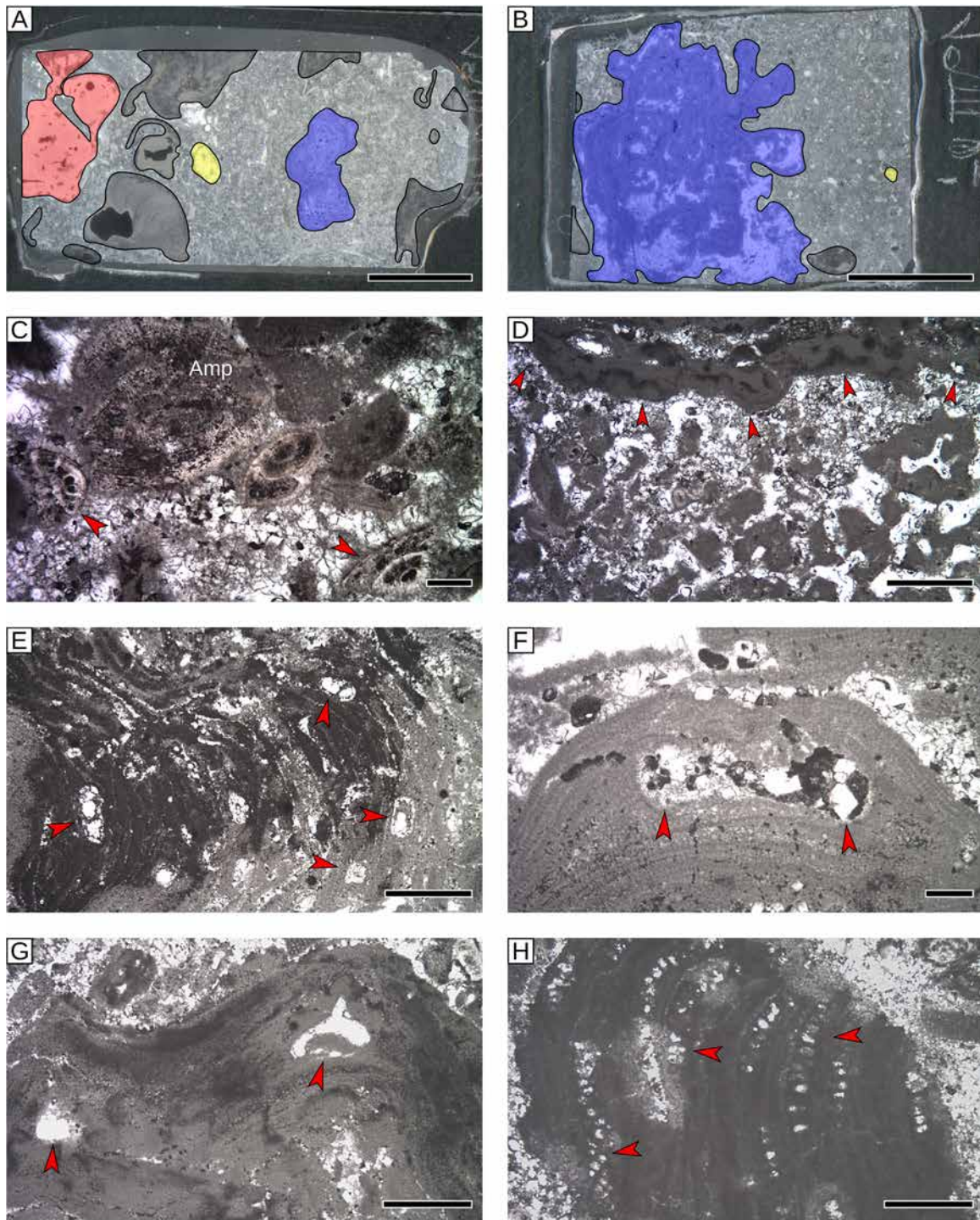


Fig. 4. Rhodolith and coral facies (core 19R-3). **A.** Coralline branches; color-coding as in Fig. 2. **B.** Branched rhodolith; color coding as in Fig. 2. **C.** Benthic foraminifera of the rhodolith and coral facies; Amp: *Amphistegina*; Red arrowheads: *Neoconorbina*. **D.** Porites fragment at the core of a rhodolith, red arrowheads indicate the base of the thallus of a Corallinales. **E.** Hapalidiales; Red arrowheads: multiporate conceptacles. **F.** Detail of a multiporate conceptacle (red arrowheads) filled by dolomite crystals. **G.** Corallinales; Red arrowheads: uniporate conceptacles. **H.** *Sporolithon*; red arrowheads: sori. Scale bars: 1 cm (A, B), 100 μm (C, F), 500 μm (D, E, G, H).

crispatum (Fig. 6(E, F)). The latter species was identified thanks to its peculiar morphology of the pore canals, which present easily recognizable pits on their outer end (Fig. 6(F)). *Mesophyllum* is common in the upper part of the interval (core 16R-2; Fig. 6(G)). Corallinales are quite common (23.5%; Figs. 5, 6(H)), and among them it is possible to recognize the genus *Titanoderma* (very distinctive due to its large cells). Sporolithales are generally rare

(5.5%) and all the observed thalli occur between cores 16R-3 and 16R-2 (Fig. 5).

4.3. Rhodolith and coral facies; 16R-1 to 15R-1

This interval is characterized by the same skeletal assemblage observed in core 19R-3 (Fig. 5). Coralline algae mainly occur as

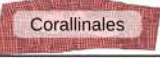
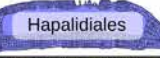
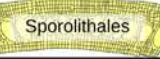
Cores	19R- 3	19R-2 to 16R-2	16R-1 to 15R-1	14R-1 to 11R-1	10R-1 to 7R-1
Facies	Rhodolith & coral	Coralline algal & <i>Heterostegina</i>	Rhodolith & coral	Coral-reef	Mollusk & benthic foraminifer
 Corallinales	35%	23.5%	14%	64%	99.5%
 Hapalidiales	63.5%	71%	68%	0%	0.5%
 Sporolithales	1.5%	5.5%	17%	36%	0%
Facies analysis, from Coletti et al., 2019					
Dunham classification	Rudstone	Wackestone to packstone	Rudstone	Rudstone or boundstone	Grainstone to wackestone
Foraminiferal assemblage	<i>Amphistegina</i> & epiphytes	<i>Heterostegina</i> & epiphytes	<i>Amphistegina</i>	Miliolids & encrusting foraminifera	Miliolids & encrusting foraminifera
Point counting of the skeletal assemblage, from Coletti et al., 2019					
Coralline algae	63.5%	63%	67%	32.5%	16%
Corals	12%	0%	21%	38%	14.5%
Benthic foraminifera	17%	29%	11%	21.5%	43%
Planktonic foraminifera	0%	1%	0%	0%	0.5%
Echinoids	7%	3.5%	0.5%	3%	4%
Mollusks	5%	2%	0%	4.5%	18%
Bryozoans	0%	0.5%	0.5%	0%	1.5%
Others	0%	1%	0%	0.5%	2.5%

Fig. 5. Coralline algal assemblage, skeletal assemblage and foraminiferal assemblage in the investigated facies of the Eratosthenes Seamount. Compositions of the skeletal and foraminiferal assemblages as well as information on the rock texture are from Coletti et al. (2019).

branching rhodoliths (dichotomous branching) with a relatively compact internal structure and small branches (Fig. 7(A)). Laminar rhodoliths are also present but they are less common than branching ones; they also have a relatively compact internal structure. The nodules are generally entirely composed of coralline algae, although locally coral fragments can be observed at the core. Thin crusts also occur but they are much less abundant than in the coralline algal and *Heterostegina* facies. Coralline-algal flora is dominated by Hapalidiales (68%) and *Mesophyllum* is by far the most common genus (Figs. 5, 7(B, C)). Sporolithales are relatively common (17%) and represent a sizable fraction of the thick branches that are frequently observed in this facies (Figs. 5, 7(D)). Corallinales also occur (14%; Fig. 5).

4.4. Coral-reef facies; 14R-1 to 11R-1

This facies is dominated by colonial corals and coralline algae. The algae mainly occur as thick branches (5 mm) and small rhodoliths (ca. 2 cm, generally branching but also laminar) with a compact internal structure (Figs. 5, 8(A)). Corallinales dominate the assemblage (64%; Fig. 5). Among them, the most common genera are *Spongites*, *Titanoderma*, and *Lithophyllum* (Fig. 8(B–E)). The identification of the former genus has been mainly based on the uniporate conceptacles (Fig. 8(B)), the presence of common fusions between cells of contiguous filaments (Fig. 8(C)), the presence of a non-coaxial hypothallus, the lack of trichocytes (Fig. 8(C)), and the pattern of development of the conceptacles characterized by cell filaments lining the outer border of the conceptacle and protruding into the pore canal (Fig. 8(D)); however, due to the imperfect preservation of the specimens, other Corallinales genera cannot be entirely excluded. Sporolithales are common (36%) and they are mainly represented by small branching rhodoliths (ca. 2 cm) and branches (either originally free-living or resulting from the fragmentation of the aforementioned rhodoliths) (Figs. 5, 8(F)). Hapalidiales are entirely absent in this facies (Fig. 5).

4.5. Mollusk and benthic foraminifer facies; 10R-1 to 7R-1

This interval is characterized by mollusks and a highly diversified foraminiferal assemblage, largely dominated by miliolids (including *Borelis*, *Dendritina* and *Spirolina*; Fig. 9(A, B)) and encrusting rotaliids. Corals and calcareous algae are also present. The algae include common coralline algae and rare green calcareous algae (Figs. 5, 9(C)). Corallines mainly occur as very small nodules (<1 cm), branches and fragments of thick crusts. Articulated coralline algae were also observed (Fig. 9(D)). Among non-geniculate corallines, the association is almost entirely composed of Corallinales (99.5%), while Hapalidiales are very rare (0.5%) and Sporolithales are absent (Fig. 5). In this facies, corallines were well preserved and, therefore, species level identification was possible.

The most common taxa are *Lithophyllum dentatum*, *Lithophyllum* sp. 1, and *Titanoderma*. *Lithophyllum dentatum* occurs as fragments of thick crusts (ca. 500 µm or more; Fig. 9(E)). The encrusting thalli comprise a central medulla in which the cells are organized in concentric arcs, surrounded by a cortex with smaller rectangular cells (Table 2; Fig. 9(E)). The organization of both medulla and the cortex are very regular (Fig. 9(E, F)). Lateral cell fusions were not observed (Fig. 9(E, F)). The observed conceptacles are quite small and have a short and conical pore-canal with a wide base (Table 2; Fig. 9(F)). The floor of the conceptacle is slightly raised (Fig. 9(F)).

Lithophyllum sp. 1 occurs as small branches (ca. 2 mm in diameter; Fig. 10(A)). The thallus has a dimerous construction and the hypothallus is composed of square to rectangular cells of similar size and shape of those of the perithallus. The perithallus has square to rectangular cells and is organized in lens-shaped growth-bands composed of two to three rows of cells (Table 2; Fig. 10(B, C)). Lateral cell fusions were not observed (Fig. 10(C)). Presumed asexuate sporangial conceptacles have a short and cylindrical pore canal (mean length ca. 65 µm and mean basal diameter ca. 30 µm) and are characterized by a raised floor

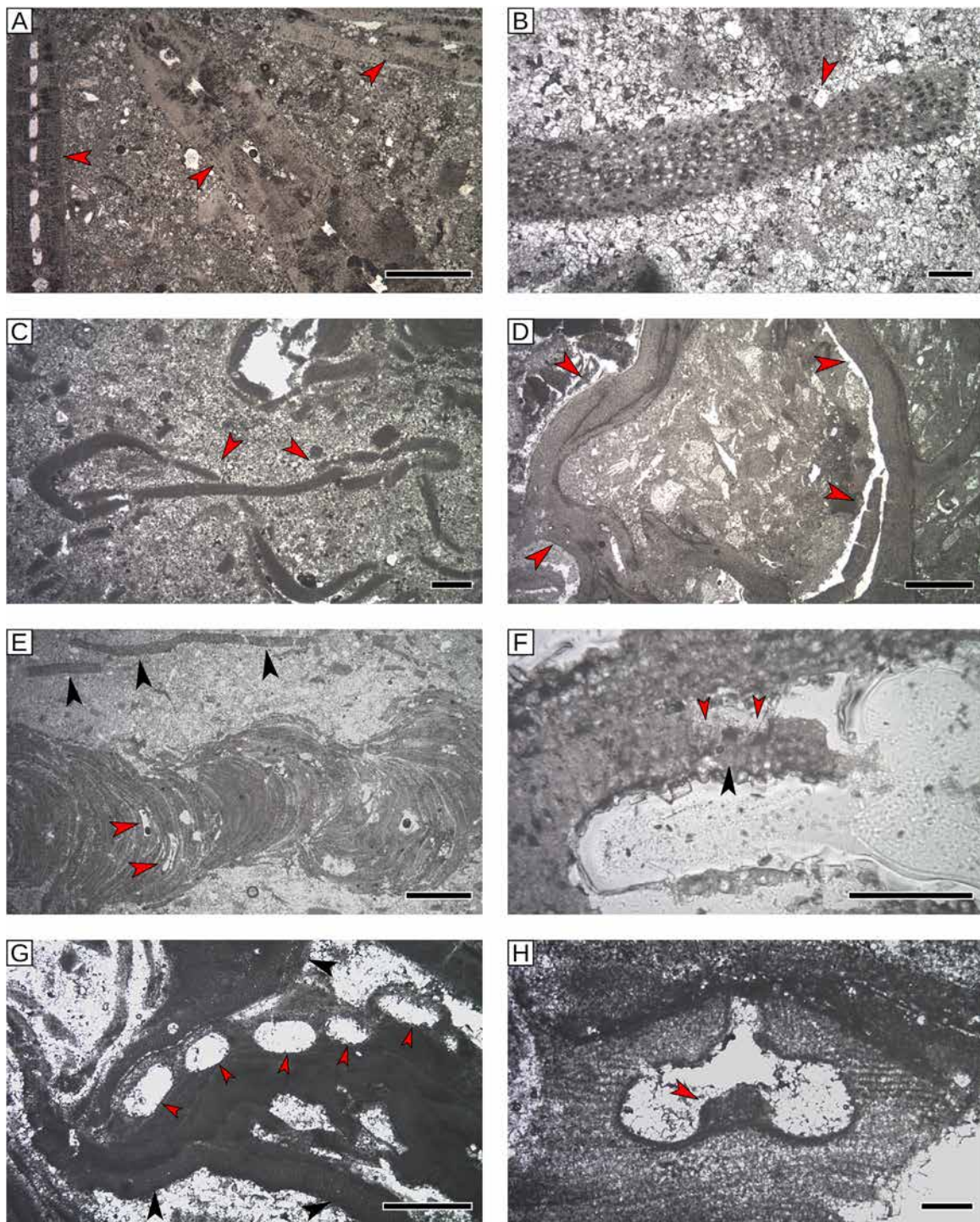


Fig. 6. Coralline algal and *Heterostegina* facies (cores 19R-2 to 16R-2). **A.** *Heterostegina* specimens (18R-2). **B.** Coralline algal crust with a coaxial hypothallus; Red arrowhead: dolomite crystal (core 17R-3). **C.** Hooked coralline algal crust (red arrowheads) (core 17R-3). **D.** Detail of an Hapalidiales nodule with a loose internal structure (core 17R-1); Red arrowhead: coralline algal crusts. **E.** Branch of *Lithothamnion crispatum* (core 17R-2); Red arrowheads: multiporate conceptacle; Black arrowheads: thin coralline algal crust. **F.** Detail of a conceptacle of *Lithothamnion crispatum* (core 18R-2); Red arrowheads: pit; black arrowhead: pore canal. **G.** *Mesophyllum* (core 16R-2); Red arrowheads: multiporate conceptacles; Black arrowheads: coaxial hypothallus. **H.** Corallinales (core 16R-2); Red arrowhead: columella within a uniporate conceptacle. Scale bars: 500 μm (A, C, G), 100 μm (B, F, H), 1 mm (D, E).

(Table 2; Fig. 10(C, D)). These conceptacles were probably raised above the surrounding thallus surface when functional and were later buried by the subsequent growth of the thallus (Fig. 10(B, C)). The presumed male gametangial thallus has an identical vegetative anatomy (Table 2). The male gametangial conceptacles are smaller and have a conical pore canal (ca. 55 μm of length and

30 μm of diameter at the base) quite large relative to the size of the conceptacle (Table 2; Fig. 10(E, F)).

Titanoderma occurs in this facies mainly as small fragments of thin encrusting thalli (composed of one to few cell rows), the latter being especially abundant in core 7R-2 (Fig. 11(A-C)). Other Corallinales, probably belonging to either Neogoniolithoideae,

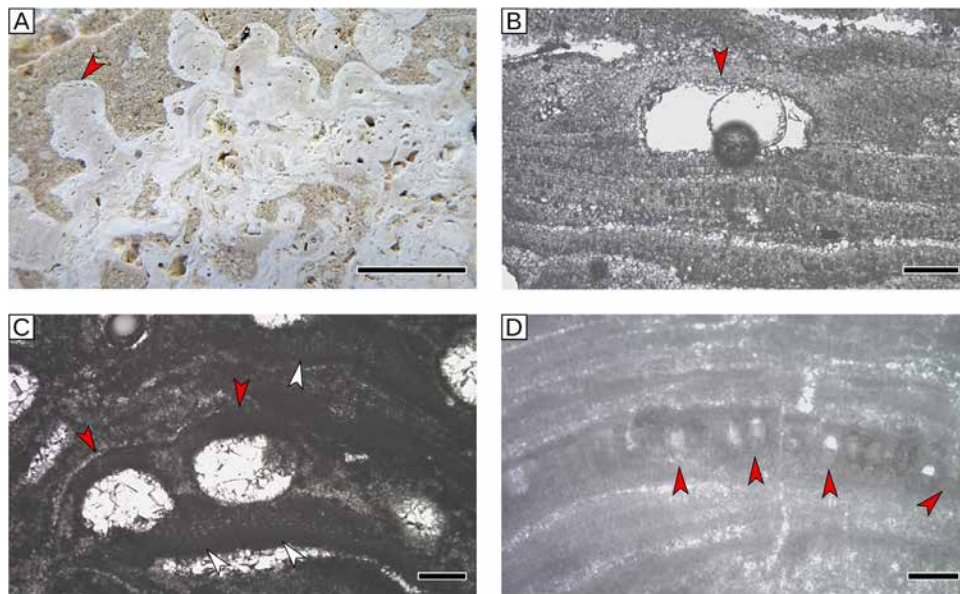


Fig. 7. Rhodolith and coral facies (cores 16R-1 to 15R-1). **A.** Branched rhodolith (core 15R-2); Red arrowhead: conceptacles. **B.** Hapalidiales (core 15R-1); Red arrowhead: multiporate conceptacle. **C.** *Mesophyllum* (core 15R-1); Red arrowheads: multiporate conceptacles; White arrowheads: coaxial hypothallus. **D.** *Sporolithon* (core 15R-2); Red arrowheads: stalk cells within sporangial compartments. Scale bars: 1 cm (A), 100 μ m (B–D).

Chamberlainoideae or Hydrolithoideae (*sensu* Caragnano et al., 2018) are also present, but they lack the features necessary for a more accurate identification (Fig. 11(D–F)).

5. Discussion

5.1. Palaeobathymetry

The presence of hermatypic colonial corals and large benthic foraminifera indicates that the Miocene succession of the Eratosthenes Seamount formed in a tropical environment (Coletti et al., 2019). The low concentrations of bioavailable phosphorus, measured with the SEDEX sequential extraction (Ruttenberg et al., 2009; Coletti et al., 2017), indicate oligotrophic conditions (Coletti et al., 2019). Consequently, the palaeobathymetric reconstruction needs to be mainly based on the comparison with coralline depth distributions from modern oligotrophic tropical environments.

The upper and lower intervals of the Miocene section characterized by the rhodolith and coral facies present almost the same skeletal assemblage (Fig. 5). The foraminiferal assemblages are also quite similar and are both characterized by the common presence of *Amphistegina* (Fig. 5). The coralline association is also similar (Fig. 5). Both assemblages are dominated by Hapalidiales associated with a relevant (15–35%) amount of Corallinales and Sporolithales (Figs. 5, 12). Generally, in tropical oligotrophic environments, Hapalidiales become a major component of the coralline-algal flora below 40 m of water depth (Adey, 1986; Minnery et al., 1985; Iryu, 1992), and below 60 m Corallinales are just minor components (Adey, 1986; Minnery et al., 1985; Iryu, 1992; Lund et al., 2000). Thus, the quantitative analysis of coralline-algal abundance would suggest a water-depth comprised between 40 and 60 m. The original estimate of 20–30 m of water-depth, proposed by Coletti et al. (2019) for the rhodolith and coral facies, was based on the elevated thickness/diameter ratio of *Amphistegina* (comprised between 0.5 and 0.6, and thus typical of very-shallow settings; Hallock and Glenn, 1986; Beavington-Penney and Racey, 2004; Mateu-Vicens et al., 2009), and on the common presence of *Porites*, while data on coralline

algal abundance were not available. A water depth of 40 to 60 m is not consistent with thick and robust specimens of *Amphistegina* and common *Porites*; however, several additional factors need to be considered. First of all, the rhodolith and coral facies is interbedded with the coralline algal and *Heterostegina* facies. Therefore, the rhodolith bed environment represented by the former is interpreted to have been adjacent to the macrophyte meadow represented by the latter (Coletti et al., 2019). The boundary between the two environments was most likely not sharp, and scattered macrophytes were probably also occurring in the rhodolith bed, thus possibly providing some shading to the seafloor favoring Hapalidiales. Second, the abundance of *Mesophyllum* (which is the most light-loving genus among Hapalidiales; Adey, 1986; Iryu, 1992; Ballesteros and Afonso-Carrillo, 1995; Cabioch et al., 1999; Basso et al., 2009) suggests that the water was not so deep. Third, although the limited extension of the core (only 6 cm of diameter) and the poor recovery do not allow to observe current or mass-transport related structures, the possibility of resedimentation cannot be ruled out, especially since the tests of *Amphistegina* are relatively small and light (few millimeters in diameter) and even relatively weak currents can displace them. Therefore, it is possible that some of the observed *Amphistegina* specimens were moved downward from shallower settings. On the other hand, rhodoliths being heavier and more resistant to transport, are more likely to represent *in situ* production. Taking this evidence into account, and based on the new quantitative data on coralline-algal assemblage, we suggest that water-depth estimate for the rhodolith and coral facies should be revised to 30–40 m of water depth (Fig. 12).

The coralline algal and *Heterostegina* facies is characterized by thin and fragile hooked crusts of coralline algae, abundant epiphytic foraminifera, very thin and flat specimens of *Heterostegina*, and rare planktonic foraminifera. Hooked coralline-algal crusts and abundant epiphytes support the interpretation of this facies as a macrophyte meadow (Brasier, 1975; Beavington-Penney et al., 2004; Sola et al., 2013; Tomassetti et al., 2016; Brandano et al., 2019). Large, flat and thin nummulitids with partitioned chambers are generally common at the lower limit of the photic zone (Hohenegger, 2000; Hohenegger et al., 2000;

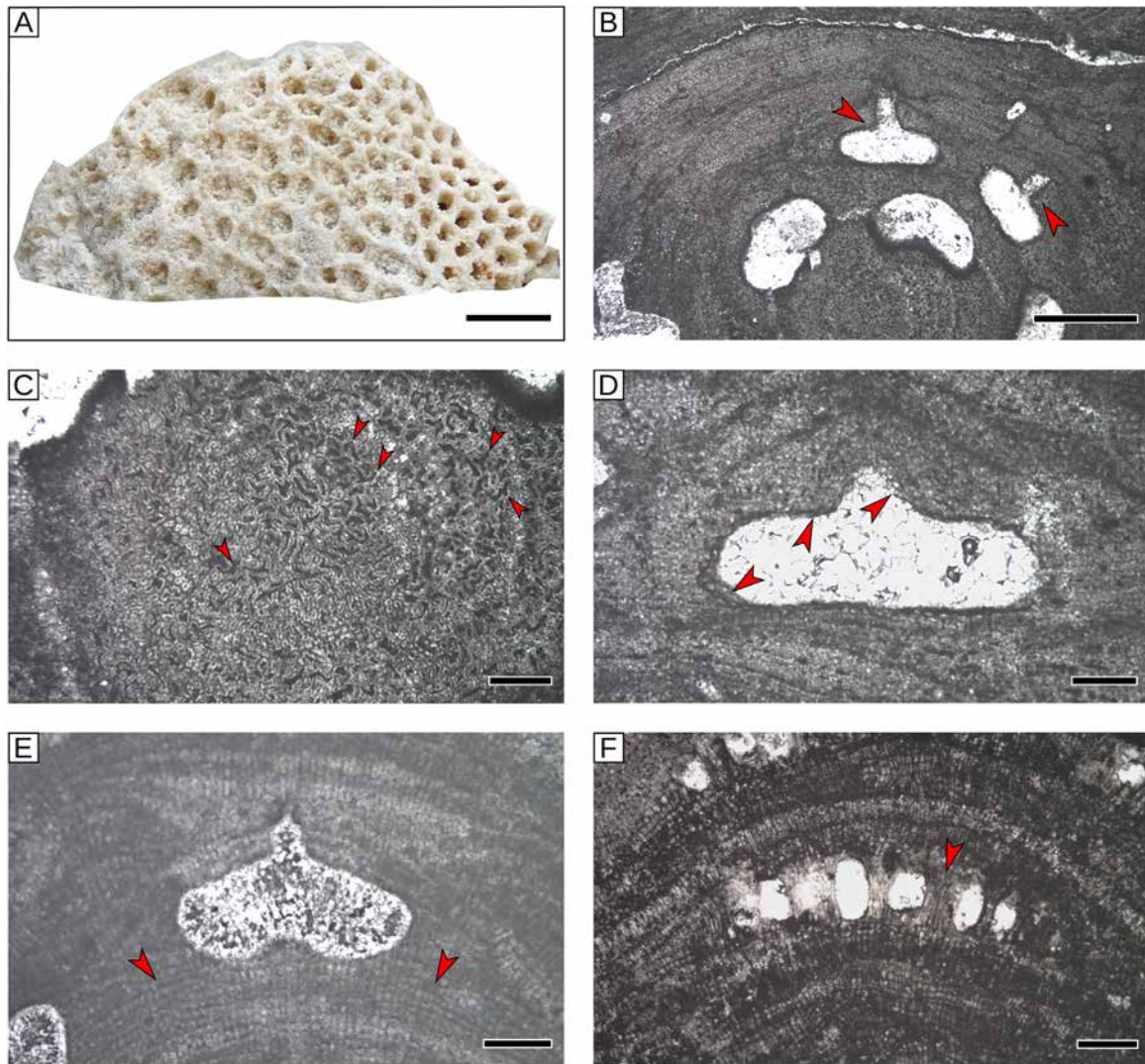


Fig. 8. Coral reef facies (cores 14R-1 to 11R-1). **A.** Colony of hermatypic corals (core 12R-1). **B.** *Spongites* (core 11R-2); Red arrowheads: uniporate conceptacles cut through the central part of the cavity. **C.** *Spongites* (core 11R-2); Red arrowheads: cell fusions. **D.** *Spongites*, detail of an uniporate conceptacle (core 11R-2); Red arrowheads: pore canal cells lining the conceptacle and protruding within the pore canal. **E.** *Lithophyllum* (core 11R-1); Red arrowheads: well preserved area of the thallus showing no cell fusions. **F.** *Sporolithon* (core 12R-1); red arrowhead: elongated cells separating sporangial compartments (paraphyses). Scale bars: 1 cm (A), 500 μm (B), 100 μm (C–F).

Renema, 2006, 2018) and their presence suggests relatively deep water. However, it should be noted that complex three-dimensional environments, such as a macrophyte meadow, can provide shaded and sheltered micro-habitats favorable for these taxa even in relatively shallow conditions (Eder et al., 2018). In the present Mediterranean Sea, on an isolated seamount similar to the Miocene setting of the Eratosthenes Seamount, macrophytes are known to occur down to 70 m (Bo et al., 2011); therefore, a water depth of 30–60 m was proposed for this interval (Coletti et al., 2019). Deeper (40–60 m) conditions were proposed close to the base, due to the presence of planktonic foraminifera (Fig. 12), whilst shallower conditions (30–40 m) were proposed for the upper part, based on the increase in sediment grain size, the thickness/diameter ratio of *Heterostegina*, and the decrease in planktonic foraminifera abundance (Fig. 12). The coralline algal assemblage supports this interpretation. The facies is dominated by Hapalidiales, but Corallinales and Sporolithales are also present (Fig. 12). *Lithothamnion* and *Lithothamnion crispatum* are more abundant at the base of the interval, while *Mesophyllum* becomes progressively more common toward the top, thus supporting the shallowing-upward trend (Fig. 12; Table S1, Appendix A). Also the coralline algal morphology supports this palaeoenvironmental interpreta-

tion. Thin (and thus very fragile) crusts dominate the lower part of the interval. Toward the top, rhodoliths with a loose internal structure become more common, suggesting a limited increase in hydrodynamic energy, sufficient to trigger rhodoliths formation, but not enough to lead to development of compact laminar-concentric growth form (Bosence, 1983b). This indicates an overall low hydrodynamic energy, with an increase toward the upper part of the interval. However, it must be stressed that both trends could be simply related to variations in the density of the macrophytes canopy.

A water depth of 10 to 20 m was proposed for the coral-reef facies based on the abundance of hermatypic coral colonies and their association with large miliolids (Coletti et al., 2019). In tropical environments, Hapalidiales are extremely rare in water shallower than 10–20 m (Adey, 1986; Minnery et al., 1985; Iryu, 1992; Cabioch et al., 1999). Consistently, Corallinales dominate the flora while Hapalidiales are entirely absent (Figs. 5, 12). While the lack of Hapalidiales is in agreement with the palaeoenvironmental interpretation of the facies, the abundance of Sporolithales (Fig. 12) is more problematic. In modern environments, Corallinales are largely represented by light-loving taxa and Hapalidiales by taxa well-adapted to dim light; Sporolithales

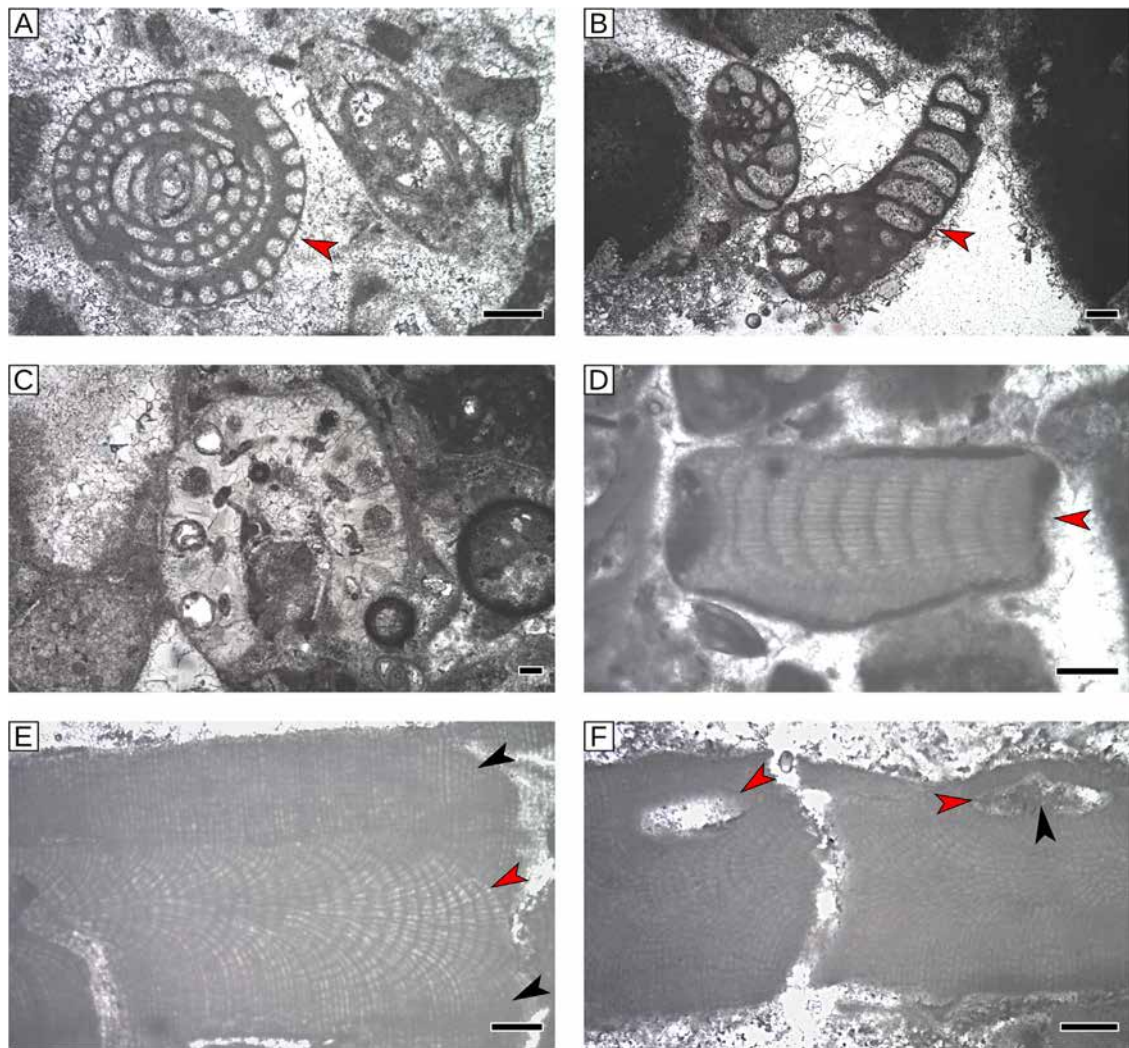


Fig. 9. Mollusk and benthic foraminifer facies (cores 10R-1 to 7R-1). **A.** Large miliolids (core 10R-1); Red arrowhead: *Borelis melo melo*. **B.** Large miliolids (core 10R-1); Red arrowhead: *Spirolina*. **C.** Green calcareous algae (core 9R-1). **D.** Articulated coralline algae (core 10R-2); Red arrowhead: intergenicula cavity. **E.** *Lithophyllum dentatum* (core 10R-1); Black arrowhead: cortex; Red arrowhead: medulla. **F.** *Lithophyllum dentatum* (core 10R-1); Red arrowheads: uniporate conceptacles; Black arrowhead: central columella. Scale bars: 100 μm .

Table 2

Biometry of *Lithophyllum dentatum* and *Lithophyllum* sp. 1 (all measurements in μm).

Taxon	Measurement	n	Mean	Standard deviation	Min	Max
<i>Lithophyllum dentatum</i>	Medulla cell diameter	63	12	1.5	9	16
	Medulla cell length	63	22	6	15	32
	Cortex cell diameter	42	12	1	9	13
	Cortex cell height	42	16	2.5	12	18
	Conceptacle diameter	4	215	25	245	295
	Conceptacle height	4	80	15	60	85
<i>Lithophyllum</i> sp. 1 sporangial	Perithallus cell diameter	78	11	1.5	9	13
	Perithallus cell height	78	14	2.6	10	21
	Conceptacle diameter	17	305	25	245	350
	Conceptacle height	17	115	15	85	140
<i>Lithophyllum</i> sp. 1 gametangial	Perithallus cell diameter	27	9.5	1	7	10
	Perithallus cell height	27	12	3	9	18
	Conceptacle diameter	3	70	7	60	75
	Conceptacle height	3	25	5	20	30

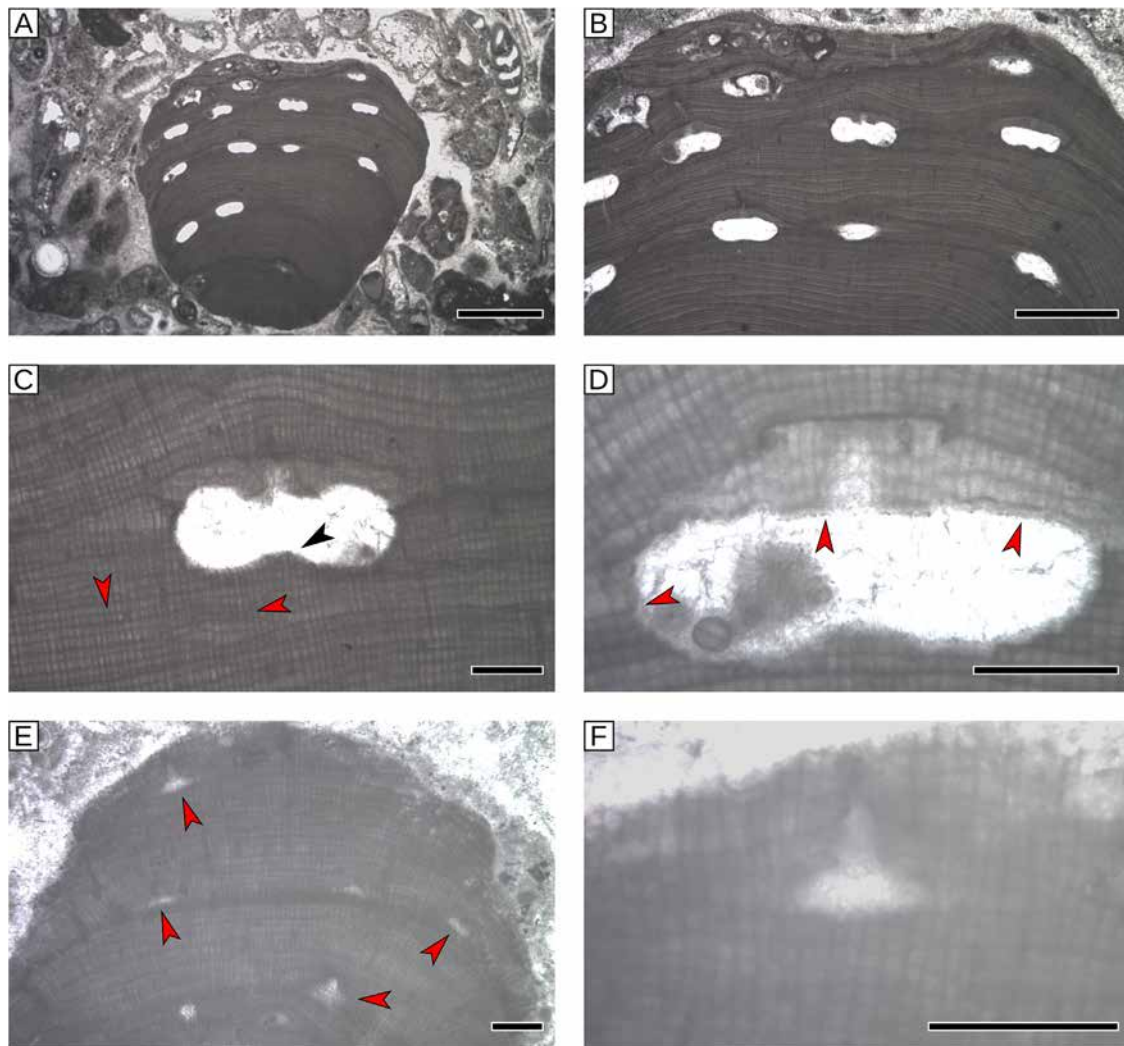


Fig. 10. *Lithophyllum* sp. 1. **A.** Branch of *Lithophyllum* sp. 1 (core 10R-2). **B.** Detail of the anatomy of the branch shown in A. **C.** Uniporate conceptacle (core 10R-2); Black arrowhead: central columella; Red arrowheads: well preserved part of thallus lacking cell fusions. **D.** Detail of a conceptacle (core 10R-2); Red arrowheads: cell filaments arranged perpendicular to the conceptacle roof and not protruding into the pore canal. **E.** Male gametangial thallus of *Lithophyllum* sp. 1 (core 10R-2); Red arrowheads: uniporate conceptacles. **F.** Detail of an uniporate conceptacle of thallus in E. Scale bars: 1 mm (A), 500 μm (B), 100 μm (C-F).

distribution is more complex. According to Lund et al. (2000), *Sporolithon* dominates at the lowest limit of photic zone. According to Rasser and Piller (1997), *Sporolithon* dominates between 20 and 40 m of water depth. Following the model of Adey (1986), Sporolithales occur in both shallow and deep settings, but they are more common in the latter, while according to Minnery et al. (1985) they mainly occur between 20 and 50 m depth. Very shallow occurrences of *Sporolithon* are also known (Basso et al., 2009; Neill et al., 2015). The geological record also presents evidence against an increase of Sporolithales with increasing water depth (Fravega et al., 1989; Brandano et al., 2005: fig. 13; Brandano et al., 2007: fig. 7; Braga et al., 2009: fig. 7; Coletti et al., 2018a: fig. 10; Chelaru et al., 2019: fig. 3). In the case of the Miocene carbonates of the Eratosthenes Seamount, Sporolithales abundance is clearly related to the proximity of the reef (Fig. 12), indicating that in this setting their distribution is mainly controlled by the presence of the suitable environment rather than by light availability. The complex distribution pattern of Sporolithales suggests that using their abundance as water-depth indicator should be avoided. The distribution of some species might be strongly correlated to water depth, but as a group they are not reliable.

On the basis of the presence of common miliolids, including shallow water genera like *Borelis*, *Dendritina* and *Spirolina* (Hallock and Glenn, 1986; Murray, 2006), a lagoonal environment with a water depth of less than 10 m was proposed for the mollusk and benthic foraminifera facies (Coletti et al., 2019) (Fig. 12). In very-shallow tropical water (<10 m of water depth), coralline-algal assemblages are almost entirely composed of Corallinales (Adey and Macintyre, 1973; Van Den Hoek et al., 1975; Minnery et al., 1985; Adey, 1986; Iryu, 1992; Rasser and Piller, 1997; Cabioch et al., 1999). Furthermore, in these settings Lithophylloideae (the sub-family of the order Corallinales encompassing those species that possess secondary pit connections) are often common and present a remarkable species diversity (Van Den Hoek et al., 1975; Iryu, 1992; Rasser and Piller, 1997). Accordingly, the coralline algal assemblage of the mollusk and benthic foraminifer facies is almost entirely composed of Corallinales and includes several lithophylloid species, the occurrence of *Lithophyllum dentatum* being particularly significant (Fig. 12). Although this species is not reported in modern tropical water, it presently inhabits the intertidal and infralittoral settings of the western Mediterranean (Bressan and Babbini, 2003). Its presence is thus consistent with a very shallow, lagoonal environment.

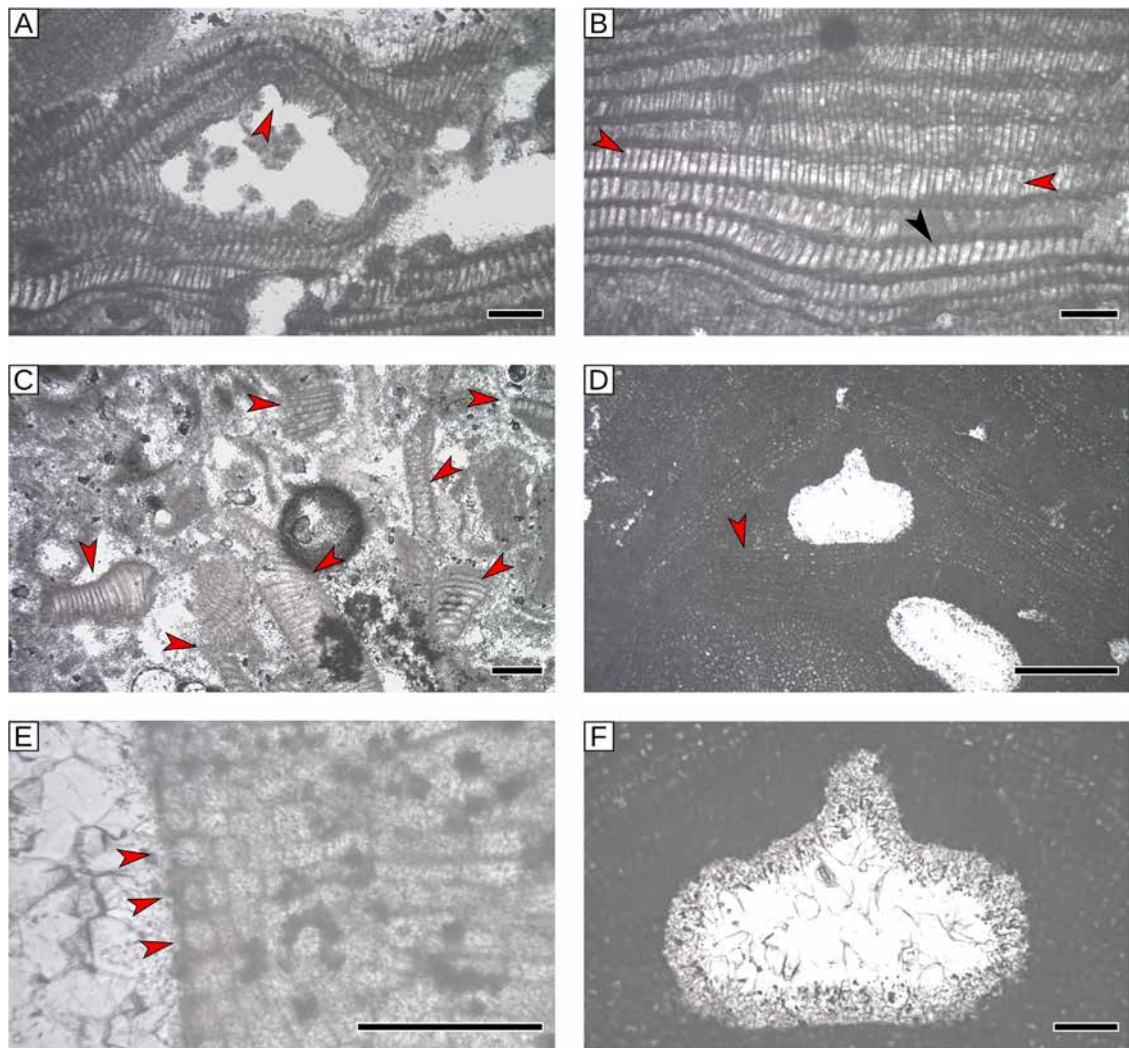


Fig. 11. Other Corallinales of the mollusk and benthic foraminifer facies. **A.** *Titanoderma* (core 10R-2); red arrowhead: oblique cut of an uniporate conceptacle not completely showing the pore canal. **B.** *Titanoderma* (core 10R-2), detail of the perithallus showing the absence of cell fusions (red arrowheads); Black arrowhead: epithallial cell. **C.** Small fragments of *Titanoderma* (core 7R-2) indicated by the red arrowheads. **D.** Corallinales sp. (core 10R-1); Red arrowhead: area of the perithallus with common cell fusions. **E.** Detail of epithallus of the same specimen shown in D; Red arrowheads: dome-shaped epithallial cells. **F.** Detail of the uniporate conceptacle shown in D. Scale bars: 100 μm (A-C, E, F), 500 μm (D).

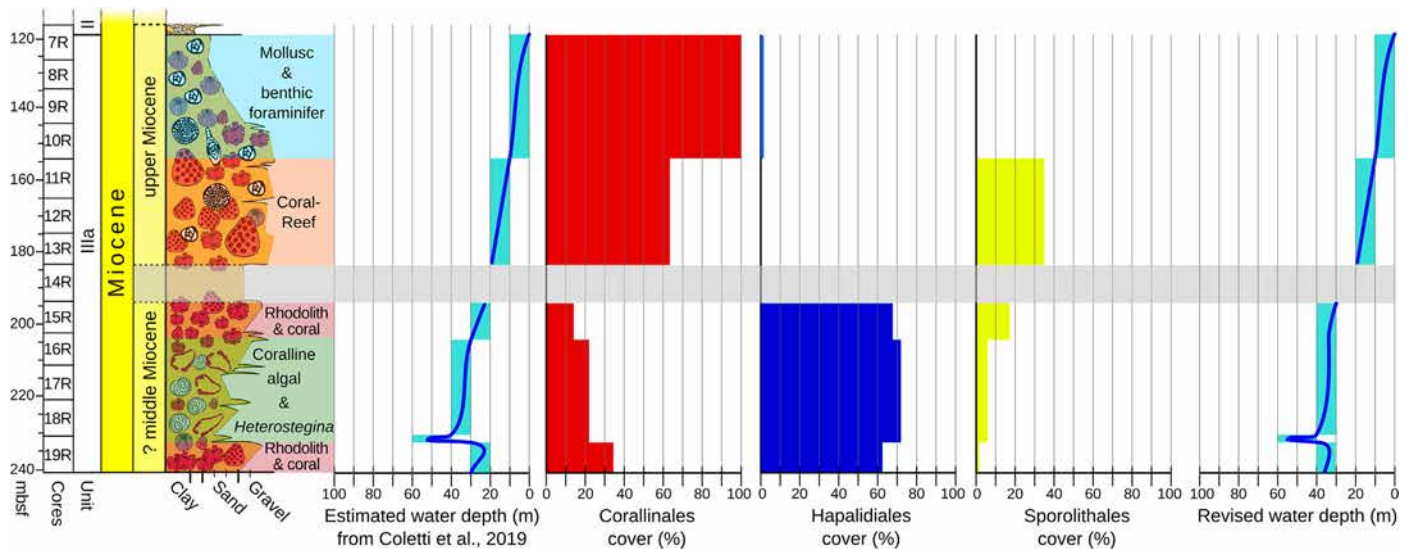


Fig. 12. Coralline-algal distribution along the studied facies, water-depth estimates based on skeletal and foraminiferal assemblages, and water-depth estimates based on coralline algal assemblage. The gray horizontal bar indicates a layer of extensive recrystallization with no preserved material; see [Coletti et al. \(2019\)](#) for further details on the diagenesis.

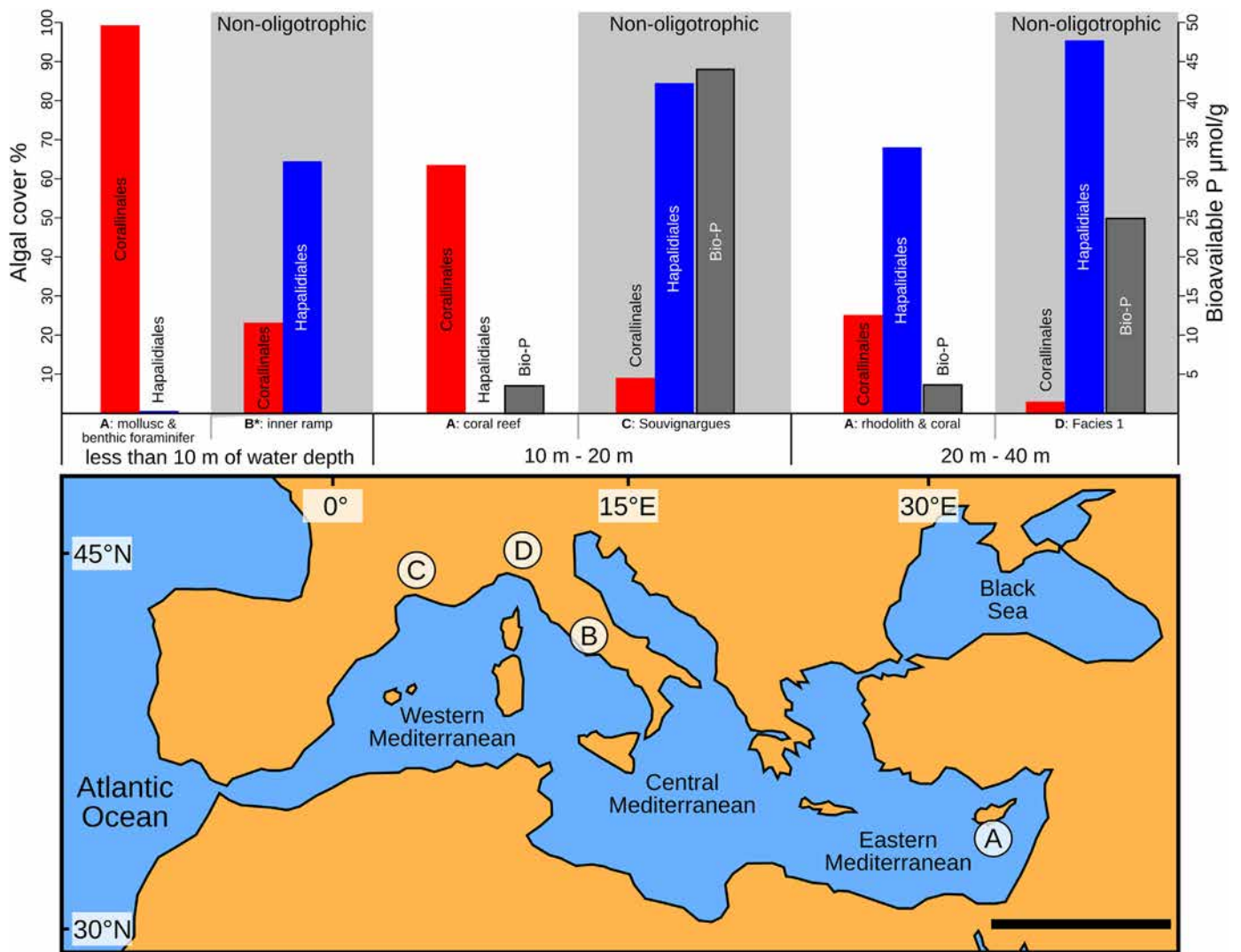


Fig. 13. Comparisons between coralline-algal distribution in oligotrophic and non-oligotrophic settings which are indicated in gray. A: Eratosthenes Seamount (values of Bio-P = bioavailable phosphorus are from Coletti et al., 2019); B: Latium-Abruzzi Carbonate Ramp, inner platform facies (data from Brandano et al., 2007); C: Souvignargues deposits of the Sommières Basin (data from Coletti et al., 2017, 2018a); D: Facies 1 of the Pietra da Cantoni limestone from the Tertiary Piedmont Basin (data from Coletti et al., 2017). Scale bar: 1000 km.

5.2. Coralline algae as depth indicators in Miocene Mediterranean carbonates

The models for coralline algal distribution proposed by Brandano et al. (2005) for the Tortonian carbonate ramp of Menorca (SE Spain) and by Braga et al. (2009) for the Messinian reefs of the western Mediterranean are the best available comparison for the middle to late Miocene facies of the Eratosthenes Seamount. The very shallow settings (<20 m) of Italian and Spanish Messinian reefs are, like those of the Eratosthenes Seamount, largely dominated ($\geq 75\%$) by Corallinales, with a remarkable abundance of taxa belonging to genera *Spongites*, *Neogoniolithon*, and *Titanoderma* (Braga et al., 2009). Conversely, Hapalidiales are almost absent (especially at water depths of <10 m; Braga et al., 2009). Furthermore, just like the Eratosthenes, coralline algae are much less common in lagoonal and back-reef facies than in the reef facies (Braga et al., 2009; Coletti et al., 2019; Fig. 5). In all three cases (Brandano et al., 2005; Braga et al., 2009; Fig. 12), in relatively shallow settings (20 to 40 m of water-depth), Corallinales abundance decreases while Hapalidiales abundance increases. Hapalidiales can even dominate (>50%) if shading is provided (e.g., by a macrophyte meadow), otherwise Corallinales

dominate. Between 40 and 60 m of water depth, Hapalidiales clearly dominate the assemblage ($\geq 75\%$), but Corallinales still occur (Brandano et al., 2005; Braga et al., 2009; Fig. 12). Below 60 m of water depth, the coralline association is almost entirely composed of Hapalidiales ($\geq 75\%$) and Corallinales are almost absent (Brandano et al., 2005; Braga et al., 2009).

These general trends are also in agreement with the palaeoenvironmental reconstruction proposed by Vescogni et al. (2014) for the middle Miocene carbonate platform of the Mut Basin of southern Turkey. These authors recognize a coral-dominated facies related to relatively shallow settings, characterized by an algal assemblage with common Hapalidiales (which are locally dominant) and common Corallinales (Vescogni et al., 2014). In the late Burdigalian Sedin platform of northern Sardinia, the distribution of coralline algae, studied along the profile of the platform clinofolds (which provides a powerful bathymetric control) is also consistent with these trends (Benisek et al., 2009). The very shallow settings (ca. 20 m) are dominated by Corallinales associated with *Sporolithon*, while moving downslope (>20 m) Hapalidiales progressively increase (Benisek et al., 2009).

In contrast to the Eratosthenes Seamount, in the Latium-Abruzzi Carbonate Ramp, Tertiary Piedmont Basin and Sommières Basin

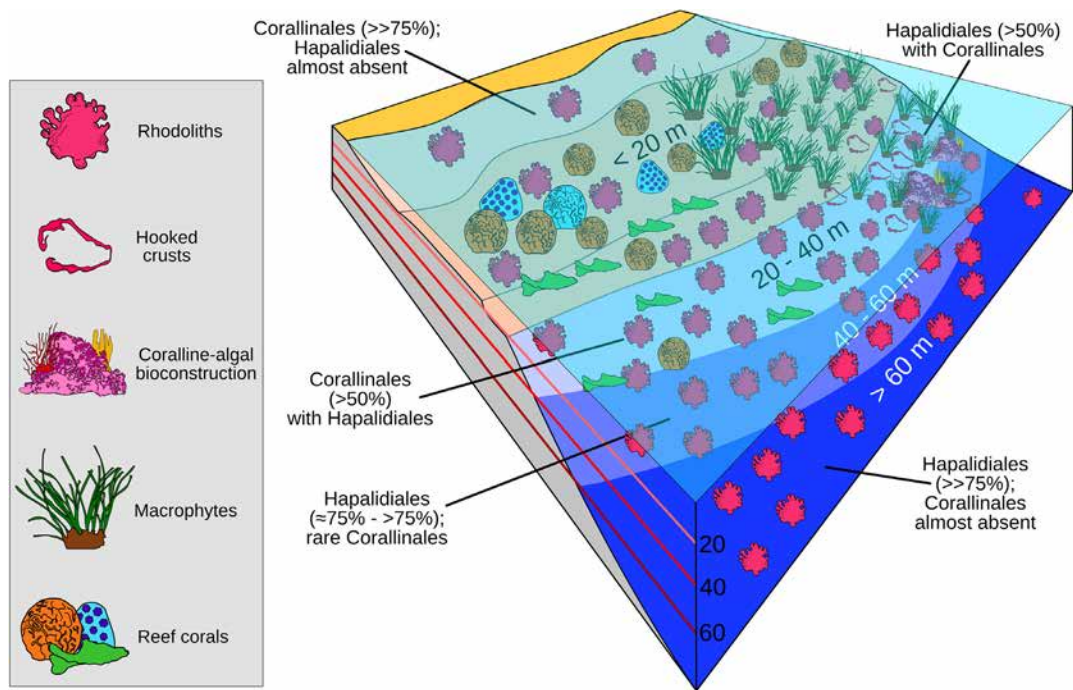


Fig. 14. Proposed model of coralline algal distribution for middle to late Miocene, tropical, oligotrophic settings. On the left side of the model is represented the hypothetical distribution of the main group of coralline algae (based on the available data) in standard carbonate systems characterized by a coral reef. On the right side is presented the difference with a carbonate system where the reef is interfingering with a macrophyte meadow (the case of the Eratosthenes Seamount), thus favoring Hapalidiales dominance already in the 20–40 m bathymetric range.

Hapalidiales clearly dominate even in very shallow settings (Brandano et al., 2007; Coletti et al., 2015, 2017, 2018a; Fig. 13). The inner ramp facies of the Latium-Abruzzi Carbonate Ramp should have formed at a water depth of <10 m (according to Mateu-Vicens et al., 2009 reconstruction based on *Amphistegina* thickness/diameter ratio) and is characterized by 64% of Hapalidiales and 23% of Corallinales (Brandano et al., 2007). The mollusk and benthic foraminifer facies of the Eratosthenes Seamount is related to a similar water depth and Hapalidiales are almost absent (Fig. 13). In the coastal deposits of Souvignargues (Sommières Basin), Hapalidiales account for 85% of the coralline flora (Coletti et al., 2017, 2018a), while they are absent in the Eratosthenes Seamount coral-reef facies (Fig. 13). The coarse-grained rhodoliths-rich deposits of the Pietra da Cantoni limestone of the Tertiary Piedmont Basin (Facies 1 *sensu* Coletti et al., 2015) are related to a water depth spanning from 20 to 40 m (based on the skeletal assemblage, in particular barnacles; Coletti et al., 2015, 2018b) and present a coralline-algal flora largely dominated by Hapalidiales (between 83% and 99%) with only minor amounts of Corallinales (1–8.5%) (Coletti et al., 2017; Fig. 13). In the rhodolith and coral facies of the Eratosthenes Seamount, which formed at a comparable water depth, Corallinales are more common (Fig. 13). The Latium-Abruzzi Carbonate Ramp, the Sommières Basin and the Tertiary Piedmont Basin were non-oligotrophic environments, as testified by the abundance of heterotroph suspension-feeders (like bryozoans and barnacles), the phosphorus concentration and the record of carbon stable isotopes (Brandano and Corda, 2002; Civitelli and Brandano, 2005; Reynaud and James, 2012; Brandano et al., 2017; Coletti et al., 2017, 2018b). Nutrient availability controls the biomass of plankton and thus the amount of particulated organic carbon in the water (Smith et al., 1981). As nutrient supply increases, the amount of organic material in the water column increases and thus water transparency decreases. Therefore, the space available for benthic phototrophs and symbiont-bearing heterotrophs (the photic zone) is reduced and the entire benthic zonation is compressed (Hallock and Schlager, 1986; Hallock, 1988, 2005; Brasier, 1995a, b; Pomar

et al., 2017). This effect fosters the dominance of Hapalidiales in shallow settings and consequently, the model of coralline algal distribution developed for oligotrophic settings cannot be used in these nutrient-rich environments. Although in non-oligotrophic settings it is also possible to observe an increase of Hapalidiales with increasing water depth (Fig. 13), the information available on the coralline-algal distribution in nutrient-rich environments are limited, thus preventing for the moment the definition in these settings of algal assemblages useful for palaeobathymetric reconstructions.

6. Conclusions

The abundance of the major coralline algal groups has been investigated and quantified in the rhodolith and coral, coralline algal and *Heterostegina*, coral-reef and mollusk and benthic foraminifer facies of the middle to late Miocene carbonate succession of the Eratosthenes Seamount. Water depth reconstructions based only on the abundance of coralline algae are similar to most of the previous estimates based on the skeletal assemblages and the benthic foraminiferal associations. Only in the rhodolith and coral facies there is a noticeable difference. The dominance of Hapalidiales is used to revise the original estimate of 20–30 m of water depth (based on the occurrence of *Porites* and the thickness/diameter ratio of *Amphistegina*) to 30–40 m. This discrepancy could be explained by different causes, such as the presence of shaded micro-habitats (favoring Hapalidiales dominance), or the downslope transport of the *Amphistegina* tests from more shallow settings.

Hapalidiales clearly increase with increasing water depth, while Corallinales decrease. On the other hand, Sporolithales abundance seems to be more tightly related to the proximity to the reef environment. Sporolithales differ from the other algal groups in that they have a more complex pattern of water-depth distribution, as suggested by several literature examples. Consequently, the ratio between Hapalidiales and Corallinales is proposed as more reliable for paleobathymetric reconstructions.

Lithophyllum dentatum mainly occurs in the lagoonal environment represented by the mollusk and benthic foraminifer facies. The presence of a modern shallow-water species strongly supports the palaeoenvironmental interpretation of this facies. This points out that, wherever possible, species level identification is extremely useful for palaeoenvironmental interpretation based on coralline algae. On the other hand, higher group distributions can be very useful at large spatial scales, such as comparing different regions.

The comparative analysis of coralline-algal distributions on the Eratosthenes Seamount, Messinian western Mediterranean reefs, and Menorca Tortonian ramp, are used to constrain several algal assemblages useful for the reconstruction of middle to late Miocene, tropical oligotrophic environments (Fig. 14). Corallinales overwhelmingly dominate the coralline association ($\geq 75\%$) in very shallow settings (0 to 20 m and especially above 10 m where Hapalidiales are almost absent). In relatively shallow conditions (20 to 40 m) Corallinales still dominate ($>50\%$), unless some sort of shading of the seafloor is present (e.g., a macrophyte meadow). Between 40 and 60 m of water depth, Hapalidiales s.l. clearly dominate the association ($\geq 75\%$), but Corallinales are still present. Below 60 m Hapalidiales overwhelmingly dominate ($\geq 75\%$) and Corallinales are almost absent. This zonation is reliable only in oligotrophic settings. In non-oligotrophic environments the coralline algal distribution is significantly different and Hapalidiales clearly dominate ($\geq 75\%$) even in very shallow settings. Therefore, tropical carbonates with abundant corals and coral-reef facies (oligotrophic) should be treated differently from those dominated by heterotroph suspension-feeders (non-oligotrophic).

These results, although preliminary and based on a relatively small dataset, highlight both the potential of reconstruction based on the quantification of coralline-algal abundance and the need for further research on coralline-algal distribution, especially in non-oligotrophic settings. The approach presented in this paper is devised to provide even a non-specialist with a simple tool to deal with coralline-algal associations and will hopefully foster new researches on distribution models for a more accurate comprehension of the past.

Acknowledgments

The authors are grateful to the International Ocean Drilling Program (IODP) for providing the samples used in this study. In particular, we thank Holger Kulmann for his assistance with sampling at the Bremen Core Repository. The authors thank Ioan Bucur and Dan Bosence for their useful suggestions and constructive revision of the manuscript, and Frédéric Quillévéré for his editorial work. Special thanks also go to Aaron Meilijson, Alastair H.F. Robertson, Dick Kroon and Silvia Spezzaferri for their useful suggestions and discussions, to Samantha Remigi and Maria Luce Frezzotti for their help with thin sections scanning, and to Curzio Malinverno for his help for thin sections preparation. This is a scientific contribution of Project MIUR – Dipartimenti di Eccellenza 2018–2022.

Appendix A. Supplementary data

Supplementary data (including Table S1) associated with this article can be found, in the online version, at <https://doi.org/10.1016/j.geobios.2020.03.005>.

- Adey, W.H., 1979. Crustose coralline algae as microenvironmental indicators in the Tertiary, in: Gray, J., Boucot, A.J. (Eds.), *Historical Biogeography, Plate Tectonics and the changing environment*. Proceedings of the thirty-seventh Annual Biology Colloquium, pp. 459-464.
- Adey, W.H., 1986. Coralline algae as indicators of sea-level, in: Van de Plassche, O. (Ed.), *Sea-level research: a manual for the collection and evaluation of data*. Geo-Books, Norwich, pp. 229-280.
- Adey, W.H., Macintyre, I.G., 1973. Crustose coralline algae: a re-evaluation in the geological sciences. *Geological Society of America Bulletin* 84, 883-904.
- Adey, W.H., Townsend, R.A., Boykins, W.T., 1982. The crustose coralline algae (Rhodophyta: Corallinaceae) of the Hawaiian Islands. *Smithsonian contribution to Marine Sciences* 15, 84 pp.
- Adey, W.H., Hernandez-Kantun, J.J., Johnson, G., Gabrielson, P.W., 2015. DNA sequencing, anatomy and calcification patterns support a monophyletic, subartic, carbonate reef-forming *Clathromorphum* (Hapalidiaceae, Corallinales, Rhodophyta). *Journal of Phycology* 51, 189-203.
- Afonso-Carrillo, J., Gil-Rodriguez, M.C., Wildpret, T.W., 1984. Estudios en las algas Corallinaceae (Rhodophyta) de las Islas Canarias. Aspectos metodologicos. *Vieraea* 13, 113-125.
- Aguirre, J., Riding, R., Braga, J.C., 2000. Diversity of coralline red algae: origination and extinction patterns from the Early Cretaceous to the Pleistocene. *Paleobiology* 26, 651-667.
- Ballesteros, E., Afonso-Carrillo, J., 1995. Species record and distribution of shallow-water coralline algae in a western Indian Ocean coral reef (Trou d'Eau Douce, Mauritius). *Botanica Marina*, 38, 203-213.
- Bassi, D., 1998. Coralline Algal Facies and their Palaeoenvironments in the Late Eocene of Northern Italy (Calcare di Nago, Trento). *Facies*, 39, 179-202.
- Basso, D. 1995. Living calcareous algae by a paleontological approach: the genus *Lithothamnion* Heydrich nom. cons. from the soft bottoms of the Tyrrhenian Sea (Mediterranean). *Rivista Italiana di Paleontologia e Stratigrafia*, 101, 349-366.
- Basso, D., 1998. Deep rhodoliths distribution in the Pontian islands, Italy, a model for paleoecology of a temperate sea. *Palaeogeography Palaeoclimatology Palaeoecology* 137, 173-187.
- Basso, D., Fravega, P., Vannucci, G., 1996. Fossil and living corallinaceans related to the Mediterranean endemic species *Lithophyllum racemus* (Lamarck) Foslie. *Facies* 35, 275-292.

- Basso, D., Fravega, P., Piazza, M., Vannucci, G., 1998. Revision and re-documentation of M. Airoidi's species of *Mesophyllum* from the Tertiary Piedmont Basin (NW Italy). *Rivista Italiana di Paleontologia e Stratigrafia*, 104, 85-94.
- Basso, D., Nalin, R., Nelson, C.S., 2009. Shallow-water *Sporolithon* rhodoliths from North Island (New Zealand). *Palaios*, 24, 92-103.
- Barattolo, F., Bassi, D., Romano, R., 2007. Upper Eocene larger foraminiferal–coralline algal facies from the Klokova Mountain (southern continental Greece). *Facies*, 53, 361-375.
- Beavington-Penney, S.J., Racey, A., 2004. Ecology of extant nummulitids and other large benthic foraminifera in paleoenvironmental analysis. *Earth Sciences Reviews*, 67, 219-265.
- Beavington-Penney, S.J., Wriarth, V.P., Woelkerling, W.J., 2004. Recognising macrophyte-vegetated environments in the rock record: a new criterion using 'hooked' forms of crustose coralline red algae. *Sedimentary Geology*, 166, 1-9.
- Ben-Avraham, Z., Ginzburg, A., Makris, J., Eppelbaum, L., 2002. Crustal structure of the Levant Basin, eastern Mediterranean. *Tectonophysics*, 346, 23-43.
- Benisek M-F., Betzler, C., Marcano, G., Mutti, M., 2009. Coralline-algal assemblages of Burdigalian platform slope: implications for carbonate platform reconstruction (northern Sardinia, western Mediterranean). *Facies*, 55, 375-386.
- Bo, M., Bertolino, M., Borghini, M., Castellano, M., Harriague, A.C., DiCamillo, C.G., Gasparini, G., Mistic, C., Povero, P., Pusceddu, A., Schroeder, K., Bavestrello, G., 2011. Characteristics of the Mesophotic Megabenthic Assemblages of the Vercelli Seamount (North Tyrrhenian Sea). *Plos One*, 6, e16357, doi:10.1371/journal.pone.0016357.
- Bosence, D.W.J., 1983a. Description and classification of rhodoliths (rodoids, rhodolites), in: Peryt, T.M. (Ed.), *Coated Grains*. Springer-Verlag, New York, pp. 217-224.
- Bosence, D.W.J., 1983b. The Occurrence and Ecology of Recent Rhodoliths - A Review, in: Peryt, T.M. (Ed.), *Coated Grains*. Springer-Verlag, New York, pp. 227-242.
- Braga, J.C., Aguirre, J., 1995. Taxonomy of fossil coralline algal species: Neogene Lithophylloideae (Rhodophyta, Corallinaceae) from southern Spain. *Palaeogeography Palaeoclimatology Palaeoecology*, 86, 265-285.
- Braga, J.C., Aguirre, J., 2001. Coralline algal assemblages in upper Neogene reef and temperate carbonates in Southern Spain. *Palaeogeography Palaeoclimatology Palaeoecology*, 175, 27-41.
- Braga, J.C., Aguirre, J., 2004. Coralline algae indicate Pleistocene evolution from deep, open platform to outer barrier reef environments in the northern Great Barrier Reef margin.

- Braga, J.C., Bosence, D.W.J., Steneck, R.S., 1993. New anatomical characteristics in fossil coralline algae and their taxonomic implications. *Paleontology* 36, 535-547.
- Braga, J.C., Vescogni, A., Bosellini, F.R., Aguirre, J., 2009. Coralline algae (Corallinales, Rhodophyta) in the western and central Mediterranean Messinian reefs. *Palaeogeography Palaeoclimatology Palaeoecology* 275, 113-128.
- Braga, J.C., Bassi, D., Piller, W.E., 2010. Paleoenvironmental significance of Oligocene-Miocene coralline red algae – a review. In: Mutti M., Piller W.E. & Betzler C. (Eds.), *Carbonate system during the Oligocene-Miocene Climatic Transition*. International Association of Sedimentologist, Special Publication 42, pp. 165-182.
- Bracchi V.A., Nalin, R., Basso, D., 2014. Paleoecology and dynamics of coralline dominated facies during a Pleistocene transgressive-regressive cycle (Capo Colonna marine terrace. Southern Italy). *Palaeogeography Palaeoclimatology Palaeoecology*, 414, 296-309.
- Brandano, M., Corda, L., 2002. Nutrients, sea level and tectonics: constraints for the facies architecture of a Miocene carbonate ramp in central Italy. *Terra Nova*, 14, 257-262.
- Brandano, M., Vannucci, G., Pomar, L., Obrador, A., 2005. Rhodolith assemblages from the lower Tortonian carbonate ramp of Menorca (Spain): Environmental and paleoclimatic implications. *Palaeogeography Palaeoclimatology Palaeoecology*, 226, 307-323.
- Brandano, M., Vannucci, G., Mateu-Vicens, G. 2007. Le alghe rosse calcaree come indicatori paleoambientali: l'esempio della rampa carbonatica Laziale-Abruzzese (Burdigaliano, Appennino centrale). *Bollettino della Società Geologica Italiana*, 126, 55-69.
- Brandano, M., Cornacchia, I., Raffi, I., Tomassetti, L., Agostini, S., 2017. The Monterey Event within the Central Mediterranean area: The shallow-water record. *Sedimentology*, 64, 286–310.
- Brandano, M., Tomassetti, L., Cornacchia, I., 2019. The lower Rupelian cluster reefs of Majella platform, the shallow water record of Eocene to Oligocene transition. *Sedimentary Geology*, 380, 21–30.
- Brasier, M.D., 1975. An outline history of seagrass communities. *Palaeontology*, 18, 681-702.
- Brasier, M.D., 1995a. Fossil indicators of nutrient levels 1: eutrophication and climate change, in: Bosence, D.W.J., Allison, P.A. (Eds.), *Marine Paleoenvironmental Analysis from Fossils*. Geological Society Special Publication 83, pp. 113–132.
- Brasier, M.D., 1995b. Fossil indicators of nutrient levels 2: evolution and extinction in relation to oligotrophy, in: Bosence, D.W.J., Allison, P.A. (Eds.), *Marine Paleoenvironmental Analysis from Fossils*. Geological Society Special Publication 83, pp. 133–150.

- Bressan, G., Babbini, L., 2003. Corallinales del Mar Mediterraneo: guida alla determinazione. *Biologia Marina Mediterranea*, Genova, 240 pp.
- Bucur, I.I., Filipescu, S., 1994. Middle Miocene red algae from the Transylvanian Basin (Romania). *Beiträge zur Paläontologie*, 19, 39-47.
- Cabioch, G., Montaggioni, L.F., Faure, G., Ribaud-Laurenti, A. Reef coralgal assemblages as recorders of paleobathymetry and sea level changes in the Indo-Pacific province. *Quaternary Science Reviews*, 18, 1681-1695.
- Caragnano, A., Foetisch, A., Maneveldt, G.W., Millet, L., Liu, L.C., Lin, S.M., Rodondi, G., Payri, C.E., 2018. Revision of Corallinaceae (Corallinales, Rhodophyta): recognizing *Dawsoniolithon* gen. nov., *Parvicellularium* gen. nov. and Chamberlainoideae subfam. nov. containing *Chamberlainium* gen. nov. and *Pneophyllum*. *Journal of Phycology*, 54, 391-409.
- Checconi, A., Bassi, D., Carannante, G., Monaco, P., 2010. Re-deposited rhodoliths in the Middle Miocene hemipelagic deposits of Vitulano (Southern Apennines, Italy): Coralline assemblage characterization and related trace fossils. *Sedimentary Geology*, 225, 50-66.
- Chelaru, R., Bucur, I.I., 2016. The taxonomy of middle Miocene red algae from the Gârbova de Sus Formation (Transylvanian Basin, Romania). *Carnets de Geologie*, 16, 307-336.
- Chelaru, R., Săsăran, E., Tămaş, T., Bălc, R., Bucur, I.I., Pleş, G., 2019. Middle Miocene carbonate facies with rhodoliths from the NW Transylvanian Basin (Vălenii Şomcutei Cave, Romania). *Facies*, 65, <https://doi.org/10.1007/s10347-018-0546-z>.
- Civitelli G., Brandano, M., 2005. Atlante delle litofacies e modello deposizionale dei Calcari a Briozoi e Litotamni nella Piattaforma carbonatica laziale-abruzzese. *Bollettino della Società Geologica Italiana*, 124, 3, 611-643.
- Cipriani, A., Fabbi, S., Lathuilière, B., Santantonio, M., 2019. A reef coral in the condensed Maiolica facies on the Mt Nerone pelagic carbonate platform (Marche Apennines): The enigma of ancient pelagic deposits. *Sedimentary Geology*, 385, 45-60.
- Coletti, G., Basso, D., Frixia, A., Corselli, C., 2015. Transported rhodoliths witness the lost carbonate factory: a case history from the Miocene Pietra da Cantoni limestone (NW Italy). *Rivista Italiana di Paleontologia e Stratigrafia* 121, 345-368.
- Coletti, G., Hrabovský, J., Basso, D., 2016. *Lithothamnion crispatum*: long-lasting species of non-geniculate coralline algae (Rhodophyta, Hapalidiales). *Carnets de Geologie*, 16, 27-41.
- Coletti, G., El Kateb, A., Basso, D., Cavallo, A., Spezzaferri, S., 2017. Nutrient influence on fossil carbonate factories: Evidence from SEDEX extractions on Burdigalian limestones (Miocene, NW Italy and S France). *Palaeogeography Palaeoclimatology Palaeoecology*, 475, 80-92.

- Coletti, G., Basso, D., Corselli, C., 2018a. Coralline algae as depth indicators in the Sommières Basin (early Miocene, Southern France). *Geobios* 51, 15-30.
- Coletti, G., Bosio, G., Collareta, A., Buckeridge, J., Consani, S., El Kateb, A., 2018b. Palaeoenvironmental analysis of the Miocene barnacle facies: case studies from Europe and South America. *Geologica Carpathica*, 69, 573-592.
- Coletti, G., Basso, D., Betzler, C., Robertson, A.H.F., Bosio, G., El Kateb, A., Foubert, A., Meilijson, A., Spezzaferri, S., 2019. Environmental evolution and geological significance of the Miocene carbonates of the Eratosthenes Seamount (ODP Leg 160). *Palaeogeography Palaeoclimatology Palaeoecology*, 530, 217-235.
- Cornacchia, I., Agostini, S., Brandano, M., 2018. Miocene Oceanographic Evolution Based on the Sr and Nd Isotope Record of the Central Mediterranean. *Paleoceanography and Paleoclimatology*, 33, 31-47.
- Dercourt, J., Gaetani, M., Vrielynck, B., Barrier, E., Biju-Duval, B., Brunet, M.F., Cadet, J.P., Crasquin, S., Sandulescu, M., 2000. Atlas Peri-Tethys, Palaeogeographical maps, 279 pp.
- Eder, W., Hohenegger, J., Briguglio, A., 2018. Test flattening in the larger foraminifer *Heterostegina depressa*: predicting bathymetry from axial sections. *Paleobiology*, 44, 76-88.
- Emeis, K.C., Robertson, A.H.F., Richter, C., et al., 1996. Proceedings of the Ocean Drilling Program, Initial Reports 160. Ocean Drilling Program, College Station, Texas, U.S.A, 972 pp.
- Feld, C., Mechie, J., Hübscher, C., Hall, J., Nicolaidis, S., Gurbuz, C., Bauer, K., Loudon, K., Weber, M., 2017. Crustal structure of the Eratosthenes Seamount, Cyprus and S. Turkey from an amphibian wide-angle seismic profile. *Tectonophysics*. 700-701, 32-59.
- Forsyth, D.W., 1980. Comparison of Mechanical Models of the Oceanic Lithosphere. *Journal of Geophysical Research*. 85, 6364-6468.
- Fravega, P., Piazza, M., Vannucci, G., 1989. *Archaeolithothamnium* Rothpletz, indicatore ecologico-stratigrafico?. Simposio di Ecologia e Paleoecologia delle Comunità Bentoniche 1985, Atti 3, 729-743.
- Halfar, J., Godinez-Orta, L., Mutti, M., Valdez-Holguin, J.E., Borges, J.M., 2004. Nutrient and temperature controls on modern carbonate production: an example from the Gulf of California, Mexico. *Geology*, 32, 213-216.
- Hallock, P., 1988. The role of nutrient availability in bioerosion: consequences to carbonate buildups. *Palaeogeography Palaeoclimatology Palaeoecology*. 63, 275-291.
- Hallock, P., 2005. Global change and modern coral reefs: New opportunities to understand shallow-water carbonate depositional processes. *Sedimentary Geology*, 175, 19-33.

- Hallock, P., Glenn, C., 1986. Larger Foraminifera: A Tool for Paleoenvironmental Analysis of Cenozoic Carbonate Depositional Facies. *Palaios*, 1, 55-64.
- Hallock, P., Schlager, W., 1986. Nutrient excess and the demise of coral reefs and carbonate platforms. *Palaios*, 1, 389–398.
- Harvey, A.S., Broadwater, S., Woelkerling, W.J., Mitrovski, P.J., 2003. *Choreonema* (Corallinales, Rhodophyta): 18S rRNA phylogeny and resurrection of the Hapalidiaceae for the subfamilies Choreonematoideae, Austrolithoideae and Melobesioideae. *Journal of Phycology*, 39, 988–98.
- Hohenegger, J., 2000. Coenoclines of larger foraminifera. *Micropaleontology*. 46, 127-151.
- Hohenegger, J., Yordanova, E., Hatta, A., 2000. Remarks on West Pacific Nummulitidae (Foraminifera). *Journal of Foraminiferal Research*. 30, 3-28.
- Hrabovský, J., 2019. Reproductive phases of Miocene algae from central Paratethys and their bearing on systematics. *Acta Palaeontologica Polonica* 64 (2): 417–439.
- Hrabovský, J., Basso, D., Doláková, N., 2015. Diagnostic characters in fossil coralline algae (Corallinophycidae: Rhodophyta) from the Miocene of southern Moravia (Carpathian Foredeep, Czech Republic). *Journal of Systematic Paleontology* 14, 499-525.
- Iryu, Y., 1992. Fossil non-articulated coralline algae as depth indicators for the Ryukyu Group. *Transactions and Proceedings of the Palaeontological Society of Japan*, 167, 1165-1179.
- Iryu, Y., Nakamori, T., Matsuda, S., Abe, O., 1995. Distribution of marine organisms and its geological significance in the modern reef complexes of the Ryukyu Islands. *Sedimentary Geology*, 99, 243-258.
- Jacobi, R.D., 1981. Peripheral bulge a causal mechanism for the Lower/Middle Ordovician unconformity along the western margin of the Northern Appalachians. *Earth and Planetary Science Letters*. 56, 245-251.
- Kinnaird, T., Robertson, A.H.F., Morris, A., 2011. Timing of uplift of the Trodos Massif (Cyprus) constrained by sedimentary and magnetic polarity evidence. *Journal of the Geological Society of London*, 168, 457-470.
- Kinnaird, T., Robertson, A.H.F., 2013. Tectonic and sedimentary response to subduction and incipient collision in southern Cyprus easternmost Mediterranean region, in: Robertson, A.H.F., Parlak, O., Ünlügenç, U.C. (Eds.), *Geological development of Anatolia and the Easternmost Mediterranean Region*. Geological Society, London, Special Publications 372. pp. 585-614.
- Kroeger, K.F., Reuter, M., Brachert, T.C., 2006. Palaeoenvironmental reconstruction based on non-geniculate coralline red algal assemblages in Miocene limestone of central Crete. *Facies*, 52, 381–409.

- Le Gall, L., Payri, C., Bittner, L., Saunders, G.W., 2009. Multigene polygenetic analyses support recognition of the Sporolithales, ord. nov. *Molecular Phylogenetics and Evolution* 54, 302-305.
- Lund, M., Davies, P.J., Braga, J.C., 2000. Coralline algal nodules off Fraser Island, Eastern Australia. *Facies* 42, 25-34.
- Major, C.O., Ryan, W.B.F, Jurado-Rodríguez, M.J., 1998. Evolution of Paleoenvironments of Eratosthenes Seamount based on downhole logging integrated with carbonate petrology and reflection profiles. In: Robertson A.H.F., Emeis K.C., Richter C., Camerlenghi A. (Eds.) - *Proceedings of the Ocean Drilling Program, Scientific Results*, 160, 483-508.
- Mart, Y., Robertson, A.H.F., 1998. Eratosthenes Seamount: an oceanographic yardstick recording the late Mesozoic-Tertiary geological history of the Eastern Mediterranean. In: Robertson A.H.F., Emeis K.C., Richter C., Camerlenghi A. (Eds.) - *Proceedings of the Ocean Drilling Program, Scientific Results*, 160, 701-708.
- Mateu-Vicens, G., Hallock, P., Brandano, M., 2009. Test shape variability of *Amphistegina d'Orbigny* 1826 as a paleobathymetric proxy: application to two Miocene examples, in: Demuchuck, T., Gary, A. (Eds.), *Geologic problems solving with microfossils. SEPM special publication* 93. pp. 67-82.
- Meilijson, I.A., Ashkenazi-Polivoda, S., Ron-Yankovich, L., Illner, P., Alsenz, H., Speijer, R.P., Almogi-Labin, A., Feinstein, S., Berner, Z., Püttmann, W., Abramovich, S., 2014. Chronostratigraphy of the Upper Cretaceous high productivity sequence of the southern Tethys, Israel. *Cretaceous Research*. 50, 187-213.
- Meilijson, A., Ashkenazi-Polivoda, S., Illner, P., Alsenz, H., Speijer, R.P., Almogi-Labin, A., Feinstein, S., Püttmann, W., Abramovich, S., 2015. Evidence for specific adaptations of fossil benthic foraminifera to anoxic–dysoxic environments. *Paleobiology*. 42, 77-97.
- Minnery, G.A., Rezak, R., Bright, T.J., 1985. Depth zonation and growth form of crustose coralline algae: Flower Garden Banks, Northwestern Gulf of Mexico, in: Toomey, D.F., Nitecki, M.H. (Eds.), *Paleoalgology: Contemporary Research and Applications*. Springer, New York, pp. 237-246.
- Montadert, L., Nicholaides, S., Semb, P.H., Lie, O., 2014. Petroleum systems offshore Cyprus. In: Marlow L., Kendall C., Yose L. (Eds.) - *Petroleum systems of the Tethyan region. AAPG memoir*, 106, 301-334.
- Murray, J.W., 2006. *Ecology and applications of benthic foraminifera*. Cambridge University Press, Cambridge.

- Murray, H., Robertson, A.H.F, 2019. Pliocene–Pleistocene sedimentary and geomorphologic development of the Vasilikos river catchment, S Cyprus, in relation to uplift of the Troodos ophiolite and climate-related changes. . Geological Magazine, <https://doi.org/10.1017/S0016756819001134>.
- Nebelsick, J.H., Stingl, V., Rasser, M., 2001. Autochthonous facies and allochthonous debris flows compared: Early Oligocene Carbonate facies patterns of the lower Inn Valley (Tyrol, Austria). *Facies*, 44: 31-46.
- Neill, K.F, Nelson, W.A., D'Archino, R., Leduc, D., Farr, T.J., 2015. Northern New Zealand rhodoliths: assessing faunal and floral diversity in physically contrasting beds. *Marine Biodiversity* 45, 63-75.
- Nelson, W.A., Sutherland, J.E., Farr, T.J., Hart, D.R., Neill, K.F., Kim, H.J., Yoon, H.S., 2015. Multi-gene phylogenetic analyses of New Zealand coralline algae *Corallinapetra novaezelandiae* gen. et sp. nov. and recognition of the Hapalidiales ord. nov. *Journal of Phycology* 51, 454-468.
- Noro, T., Masaki, T., Akioka, H., 1983. Sublittoral distribution and reproductive periodicity of crustose coralline algae (Rhodophyta, Cryptonemiales) in southern Hokkaido, Japan. *Bulletin Faculty of Fisheries Hokkaido University*, 34, 1-10.
- Perrin, C., Bosence, D.W.J., Rosen, B., 1995. Quantitative approaches to palaeozonation and palaeobathymetry of corals and coralline algae in Cenozoic reefs, in: Bosence, D.W.J., Allison, P.A. (Eds.), *Marine Palaeoenvironmental Analysis from Fossils*. Geological Society Special Publication 83, pp. 181-229.
- Perrin, C., 2000. Changes of paleozonation patterns within Miocene coral reefs, Gebel Abu Shaar, Gulf of Suez, Egypt. *Lethaia* 33, 253-268.
- Premoli-Silva, I., Spezzaferrri, S., D'Angelantonio, A., 1998. Cretaceous foraminiferal bio-isotope stratigraphy of Hole 967E and Paleogene planktonic foraminiferal biostratigraphy of Hole 966F, Eastern Mediterranean. In: Robertson A.H.F., Emeis K.C., Richter C., Camerlenghi A. (Eds.) - *Proceedings of the Ocean Drilling Program, Scientific Results*, 160, 377-394.
- Pomar, L., Morsili, M., Hallock, P., Bádenas, B., 2012. Internal waves, an under-explored source of turbulence events in the sedimentary record. *Earth-Science Reviews*, 111, 56–81.
- Pomar, L., Baceta, J.I., Hallock, P., Mateu-Vicens, G., Basso, D., 2017. Reef building and carbonate production modes in the west-central Tethys during the Cenozoic, *Marine and Petroleum Geology*, 83, 261-304.

- Quaranta, F., Vannucci, G., Basso, D., 2007. *Neogoniolithon contii* comb nov based on the taxonomic re-assessment of Mastrorilli's original material from the Oligocene of NW Italy (TPB). *Rivista Italiana di Paleontologia e Stratigrafia* 113, 43-55.
- Quaranta, F., Tomassetti, L., Vannucci, G., Brandano, M., 2012. Coralline algae as environmental indicators: a case study from the Attard member (Chattian, Malta). *Geodiversitas*, 34, 151-166.
- Rasser, M.W., Nebelsick, J.H. 2003. Provenance analysis of Oligocene autochthonous and allochthonous coralline algae: a quantitative approach towards reconstructing transported assemblages. *Palaeogeography Palaeoclimatology Palaeoecology*, 201, 89-111.
- Rasser, M.W., Piller, W.E., 1997. Depth distribution of calcareous encrusting associations in the northern Red Sea (Safaga, Egypt) and their geological implications. *Proceedings of the 8th international Coral Reef Symposium*, 743-748.
- Rasser, M.W., Piller, W.E., 1999. Application of neontological taxonomic concepts to Late Eocene coralline algae (Rhodophyta) of the Austrian Molasse Zone. *Journal of Micropaleontology*, 18, 67-80.
- Rasser, M.W., Piller, W.E., 2000. Designation of *Phymatolithon* (Corallinaceae, Rhodophyta) in fossil material and its paleoclimatological indications. *Micropaleontology*, 46, 89-95.
- Renema, W., 2006. Large benthic foraminifera from the deep photic zone of a mixed siliciclastic-carbonate shelf off East Kalimantan, Indonesia. *Marine Micropaleontology*. 58, 73-82.
- Renema, W. 2018. Terrestrial influence as a key driver of spatial variability in large benthic foraminiferal assemblage composition in the Central Indo-Pacific. *Earth Sciences Review*. 177, 514-544.
- Reynaud, J.Y., James, N.P., 2012. The Miocene Sommières basin, SE France: bioclastic carbonates in a tide dominated depositional system. *Sedimentary Geology* 282, 360-373.
- Riosmena-Rodríguez R. (2017) – Natural History of Rhodolith/Maërl Beds: Their role in near-shore biodiversity and management. In: Riosmena-Rodríguez R., Nelson W. & Aguirre J. (Eds.) – *Rhodolith/Maërl Beds: A Global Perspective*. Coastal Research Library 15, Springer, pp. 3-27.
- Robertson, A.H.F., 1998a. Lithofacies evidence for the Cretaceous-Paleogene sedimentary history of Eratosthenes Seamount, Eastern Mediterranean, in its regional tectonic context (Sites 966 and 967). In: Robertson A.H.F., Emeis K.C., Richter C., Camerlenghi A. (Eds.) - *Proceedings of the Ocean Drilling Program, Scientific Results*, 160, 403-417.
- Robertson, A.H.F., 1998b. Miocene shallow-water carbonates on the Eratosthenes Seamount, easternmost Mediterranean Sea. In: Robertson A.H.F., Emeis K.C., Richter C., Camerlenghi A. (Eds.) - *Proceedings of the Ocean Drilling Program, Scientific Results*, 160, 419-436.

- Robertson A.H.F., 1998c. Tectonic significance of the Eratosthenes Seamount: a continental fragment in the process of collision with a subduction zone in the eastern Mediterranean (Ocean Drilling Program Leg 160). *Tectonophysics*, 298, 63-82.
- Robertson, A.H.F., 1998d. Late Miocene Paleoenvironments and tectonic setting of the southern margin of Cyprus and the Eratosthenes Seamount, in: Robertson, A.H.F., Emeis, K.C., Richter, C., Camerlenghi, A. (Eds.), *Proceedings of the Ocean Drilling Program, Scientific Results 160*. pp. 453-463.
- Robertson, A.H.F., Dixon, J.E., 1984. Introduction: aspects of the geological evolution of the Eastern Mediterranean. In: Dixon J.E., Robertson A.H.F. (Eds.) - *The Geological evolution of the Eastern Mediterranean*. Geological Society Special Publication, 17, Geological Society, London, 1-74.
- Robertson, A.H.F., Eaton, S., Follows, E.J., McCallum, J.E., 1991. The role of local tectonics versus global sea-level change in the Neogene evolution of Cyprus margin, in Macdonald, D.I.M (Ed.), *Sedimentation, Tectonics and Eustasy: Sea-level changes at active Margins*. Special Publication of the International Association of Sedimentologists 12. pp. 331-339.
- Rögl F. (1999) – Mediterranean and Paratethys facts and hypotheses of an Oligocene to Miocene paleogeography (short overview). *Geologica Carpathica*, 50, 339-349.
- Rösler, A., Perfectti, F., Peña, V., Braga, J.C., 2016. Phylogenetic relationships of corallinaceae (Corallinales, Rhodophyta): taxonomic implications for reef-building corallines. *Journal of Phycology*, doi: 10.1111/jpy.12404.
- Ruttenberg, K.C., 1992. Development of a sequential extraction method for different form of phosphorus in marine sediments. *Limnology and Oceanography*, 37, 1460–1482.
- Ruttenberg, K.C., 2004. The global phosphorus cycle. In: Holland, H.D., Turekian, K.K. (Eds.), *Treatise on Geochemistry* 8, New York, Elsevier, pp. 585-643.
- Ruttenberg, K.C., Ogawa, N.O., Tamburini, F., Briggs, R.A., Colasacco, N.D., Joyce, E., 2009. Improved, high throughput approach for phosphorus speciation in natural sediments via the SEDEX sequential extraction method. *Limnology and Oceanography Methods*, 7, 319–333.
- Sañé, E., Chiocci, F.L., Basso, D., Martorelli, E., 2016. Environmental factors controlling the distribution of rhodoliths: an integrated study based on seafloor sampling, ROV and side scan sonar data, offshore the W-Pontine Archipelago. *Continental Shelf Research*, 129: 10-22.
- Sola, F., Braga, J.C., Aguirre, J., 2013. Hooked and tubular coralline algae indicate seagrass beds associated to Mediterranean Messinian reefs (Poniente Basin, Almeria, SE Spain). *Palaeogeography, Palaeoclimatology, Palaeoecology*, 374, 218–229.

- Smith, S.V., Kimmerer, V.J., Laws, E.A., Brock, R.E., Walsh, T.W., 1981. Kaneohe Bay sewage diversion experiment perspective, on ecosystem responses to nutritional perturbation. *Pacific Science*, 35, 279-395.
- Spezzaferri, S., Cita, M.B., McKenzie, J.A., 1998. The Miocene/Pliocene boundary in the Eastern Mediterranean: results from Sites 967 and 969. In: Robertson A.H.F., Emeis K.C., Richter C., Camerlenghi A. (Eds.) - *Proceedings of the Ocean Drilling Program, Scientific Results*, 160, 9-28.
- Spezzaferri, S., Tamburini, F., 2007. Paleodepth variations on the Eratosthenes Seamount (Eastern Mediterranean): sea-level changes or subsidence?. *eEarth Discuss*, 2, 115–132.
- Staerker, T.S., 1998. Data report: biostratigraphy of Eocene and Upper Cretaceous chalks from the Eratosthenes Seamount region in the Eastern Mediterranean. In: Robertson A.H.F., Emeis K.C., Richter C., Camerlenghi A. (eds.) - *Proceedings of the Ocean Drilling Program, Scientific Results*, 160, 395-401.
- Tomassetti, L., Benedetti, A., Brandano, M., 2016. Middle Eocene seagrass facies from Apennine carbonate platforms (Italy). *Sedimentary Geology*, 335, 136-149.
- Van Den Hoek, C., Cortel-Breeman, A.M., Wanders, J.B.W., 1975. Algal zonation in the fringing coral reef of Curaçao, Netherlands Antilles, in relation to zonation of corals and gorgonians. *Aquatic Botany*, 1, 269-308.
- Van Der Merwe, E., Miklasz, K., Channing, A., Maneveldt, G.W., Gabrielson, P.W. 2015. DNA sequencing resolves species of *Spongites* in the Northeast Pacific and South Africa, including *S. agulhensis* sp. nov. *Phycologia*, 54, 471-490.
- Vannucci, G., Quaranta, F., Basso, D., 2008. Revision and redocumentation of M. Airoidi species of *Lithophyllum* from the Tertiary Piedmont Basin. *Rivista Italiana di Paleontologia e Stratigrafia* 114, 515-528.
- Vescogni, A., Bosellini, F.R., Cipriani, A., Gürler, G., Ilgar, A., Paganelli, E. 2014. The Dağpazarı carbonate platform (Mut Basin, Southern Turkey): Facies and environmental reconstruction of a coral reef system during the Middle Miocene Climatic Optimum. *Palaeogeography, Palaeoclimatology, Palaeoecology*, 410, 213–232.
- Wilson, M.E.J., Vecsei, A., 2005. The apparent paradox of abundant foramol facies in low latitudes: their environmental significance and effect on platform development . *Earth-Science Reviews*, 69, 133-168.
- Woelkerling, W.J., Irvine, L.M., 1986. The typification and status of *Phymatolithon* (Corallinaceae, Rhodophyta). *British phycological journal*, 21, 55-80.

Woelkerling, W.J., Irvine, L.M., Harvey, A.S., 1993. Growth-forms in non-geniculate coralline red algae (Corallinales, Rhodophyta). *Australian Systematic Botany*, 6, 277-293.

Woelkerling, W.J., Granier, B., Dias-Brito, D., 2014. *Heydrichia* (?) *poignantii*, sp. nov (Sporolithaceae, Sporolithales, Rhodophyta), a 100 million year old fossil coralline red alga from north-eastern Brazil, and a new Hauterivian record of *Sporolithon* from Switzerland. *Carnets de Geologie*, 14, 139-158.